Article:

Shang, J, West, LJ, Hencher, SR et al. (1 more author) (2018) Geological discontinuity persistence: Implications and quantification. Engineering Geology, 241. pp. 41-54. ISSN 0013-7952

https://doi.org/10.1016/j.enggeo.2018.05.010

Geological discontinuity persistence: Implications and quantification

J. Shang[1], L. J. West[2], S. R. Hencher[2,3,4], Z. Zhao[1]

1. Nanyang Centre for Underground Space, School of Civil and Environmental Engineering, Nanyang Technological University, Singapore.

2. Engineering Geology and Hydrogeology Group, School of Earth and Environment, University of Leeds, Leeds, United Kingdom.

3. Department of Earth Sciences, University of Hong Kong, Hong Kong SAR, China

4. Hencher Associates Limited, Ilkley, United Kingdom.

Abstract

Persistence of geological discontinuities is of great importance for many rock-related applications in earth sciences, both in terms of mechanical and hydraulic properties of individual discontinuities and fractured rock masses. Although the importance of persistence has been identified by academics and practitioners over the past decades, quantification of areal persistence remains extremely difficult; in practice, trace length from finite outcrop is still often used as an approximation for persistence. This paper reviews the mechanical behaviour of individual discontinuities that are not fully persistent, and the implications of persistence on the strength and stability of rock masses. Current techniques to quantify discontinuity persistence are then examined. This review will facilitate application of the most applicable methods to measure or predict persistence in rock engineering projects, and recommended approaches for the quantification of discontinuity persistence. Furthermore, it demonstrates that further research should focus on the development of persistence

quantification standards to promote our understanding of rock mass behaviours including strength, stability and permeability.

Keywords: Discontinuity persistence; incipient discontinuity; rock bridges; geophysics; rock mass strength

1. Introduction

Geological discontinuities are of great importance for strength, deformability and permeability of rock masses. Characterisation of discontinuity geometry (i.e. aperture, persistence, length and spatial connectivity) is the first step to understanding the overall behaviour of rock masses. Early references to discontinuity persistence include those of Jennings (1970) and Einstein et al. (1983), and the summary publication by the International Society for Rock Mechanics and Rock Engineering (ISRM, 1978).

It is difficult to quantify true persistence due to the intrinsic three-dimensional nature of discontinuities within rock masses and the number of studies that have attempted to quantify this parameter has been relatively small. Some techniques have been developed in recent years, for example, geophysical detection (e.g. Heike et al., 2008; Deparis et al., 2011), surface terrestrial laser scanning (e.g. Sturzenegger and Stead, 2009a; Tuckey and Stead, 2016) and the forensic excavation of rock masses (e.g. Shang et al., 2017a). Modelling the inevitable uncertainty in the fracture network is addressed in FracMan by Diershowitz and colleagues at Golder Associates and by Monte-Carlo simulation (e.g. Wang et al., 2016)

The purpose of this paper is to consider the implications of discontinuity persistence on the mechanical properties of individual discontinuities, strength and stability of rock masses and to review the available techniques to quantity this parameter. Several recommendations for future research are included in this paper.

2. Definition

2.1 Incipient and mechanical geological discontinuities

Geological discontinuity is normally recognised as a general term to describe any mechanical break (lacking significant tensile strength) within rock masses, including most joints, weak bedding planes, weakness zones and faults (ISRM, 1978). This definition however does not apply to incipient traces, regardless of strength, although such traces are often recorded during discontinuity logging in the outcrop (Hencher, 2014 and 2015). This common practice leads to underestimation of strength of rock masses, and overestimation of permeability. It can considerably increase expenditure on rock support systems and also influence reliable prediction of water, oil and gas extraction. As a first step, it is therefore practically and theoretically important to differentiate the degree of incipiency of discontinuities in terms of their tensile strength (Hencher, 2014; Shang et al., 2016).

Incipient discontinuities may have considerable tensile strength as a result of their partial development, secondary mineralization or cementation. This concept is illustrated by Fig. 1, in which a sub-vertical incipient rock joint terminates in rock. Characterising the horizontal traces, would generally be disregarded in rock mass characterisation, but these clearly represent a weakness.

Incipient rock discontinuities often develop over geological time into full mechanical discontinuities (Hencher, 2014) with zero tensile strength as defined by ISRM (1978). Fig. 2 shows rock cores with strong incipient traces and zero-tensile strength mechanical joints; these discontinuities can be differentiated on the basis of relative tensile strength of the parent rock (Hencher, 2014; Shang et al., 2015, 2016). Fig. 3 shows different development stages of incipient joints on a face cut by a diamond wire saw. Joints can be seen as linear traces stained with iron oxides. These joints were evidently formed from brittle fracture propagation at a late stage during cooling/emplacement of this granite, as can be interpreted from cross-cutting relationships and the geometrical association of some joints with mineral differentiation (as indicated by 1, in an area washed clean with water). Note that some of the joint traces terminate as visible features, as indicated at 2. Note that one of the shallowly dipping joints, has an open aperture locally (indicated by 3) allowing seepage of groundwater, indicating partial development to a full mechanical discontinuity. Hence, it is proposed that the incipient joint pattern represents a 'blueprint' that, given time and appropriate conditions, will develop as interconnecting true, mechanical discontinuities in the sense defined by ISRM (1978).

2.2 Rock bridge and discontinuity persistence

The term 'rock bridge' is defined as an area of intact/strong rock material separating coplanar or non-coplanar discontinuities in rock masses (Kim et al., 2007b; Zheng et al., 2015). Rock bridges usually occupy a part of the planar joint plane (Dershowitz and Einstein 1988); such rock bridges in coplanar joints are the focus of this review.

True discontinuity persistence is the areal extent of a rock discontinuity. Fig. 4a illustrates the areal discontinuity persistence (K), which is defined as the fraction of continuous discontinuity area (Einstein et al., 1983) whereby:

$$K = \sum[(A_{\mathrm{D}} - A_{\mathrm{Bi}})\,/A_{\mathrm{D}}] \tag{1}$$

where $\sum A_{\mathrm{Bi}}$ is the total area of scattered rock bridges and A_{D} is reference gross area including rock bridges and continuous joint segments.

The above definition implies that a planar discontinuity follows a predefined weakness plane. For this type of geometry, the effects of the incipient parts of the discontinuity represented by rock bridges have been investigated in stability analysis. For example in a recent work reported by Viviana et al. (2015), effects of the spatially distributed rock bridges along a preferential sliding plane was investigated. In reality, however, linear persistence (K_L), see Fig. 4b, is often used as an approximation of areal persistence (Einstein et al., 1983); this is defined as a linear ratio of sum of joint segments ($\sum J_i$) and the total length of coplanar given line $\sum(J_i + B_i)$:

$$K_L = \sum \ [J_i/(J_i + B_i)] \tag{2}$$

This definition has been widely used in experimental, analytical and numerical studies (e.g. Lajtai, 1969a,b; Jennings, 1970; Zhang et al., 2006; Prudencio and Van Sint Jan, 2007; Ghazvinian et al., 2012; Bahaaddini et al., 2013; Shang et al., 2013; Jiang et al., 2015).

ISRM (1978) suggested a classification scheme for persistence by measuring length (L) of joint trace formed by the intersection of a joint within an exposure. In that scheme, five categories comprising very low persistence (L < 1 m), low persistence (1 m < L < 3 m), medium persistence (3 m < L < 10 m), high persistence (10 m < L < 20 m) and very high persistence (20 m < L) were provided. That scheme however only provides a description of discontinuities on a finite rock exposure (Norbury, 2010) and ignores the problem of joint sections that maintain strength.

The above definitions (based on coplanar discontinuities) mainly focus on the geometrical properties of single discontinuities without consideration of stress concentration around fracture tips (Kevin, 1980; Wasantha et al., 2014). Some studies considered the stress influence on degree of discontinuity persistence:

Wasantha et al. (2014) is an example in which a new parameter was developed to define persistence, considering stress distributions, however it is still difficult for the practical application in rock engineering. It is noted that there is also a difference (in definitions of persistence) between industries and universities (for example, nearly four decades ago, the term “joint continuity”, rather than “persistence”, was used in the joint survey in the Feitsui Reservoir Project, Taiwan, which is probably due to its simplicity). In this review, the term “areal persistence” (Eq. 1), reflecting the three dimensional nature of discontinuities, is recommended to be used to describe discontinuity which is the best measure of persistence.

3. Mechanical properties of individual discontinuities

Tensile or shear failure of incipient discontinuities is often the ‘final straw’ leading to instability of rock masses, which usually occurs in response to a number of triggers including temperature and insolation (Brian and Greg, 2016), precipitation (Wieczorek and Jager, 1996), weathering (Borrelli et al., 2007; Tating et al., 2013; Goudie, 2016) and seismic loading (Cravero and Labichino, 2004). In exposures and tunnel roofs, many overhanging and threatening rock blocks or slabs (Fig. 5) only remain in place because of the strength of incipient discontinuities mainly arising from rock bridges (Paolo et al., 2016). The area of rock bridge can only be viewed after collapse (see for example in Fig. 6) when strength of revealed bridges can be back analysed (Paronuzzi and Serafini, 2009).

Shang et al. (2016 and 2017c) investigated the tensile strength of incipient rock discontinuities in the laboratory. They demonstrated that incipient traces can have considerable tensile strength, and can be differentiated using relative tensile strength to that of parent rock, as originally proposed by Hencher (2014). Based on the laboratory findings by Shang et al. (2015 and 2016), a further numerical investigation of the direct tensile behaviour of laminated and transversely isotropic rocks was recently presented by Shang et al. 2017b, in which the incipiency of bedding planes (relative tensile strength to that of parent rock) was considered.

Many investigations have been undertaken to measure the shear strength of discontinuities, mostly focusing on mechanical discontinuities with zero true cohesion (Barton, 1976). For non-filled and non-persistent rock joints, shear strength is however controlled by four components including fundamental shear strength of rock bridges (Shang and Zhao, 2017), internal friction in solid bridges (after rock bridges are mobilized), friction from the persistent joint segments (Lajtai, 1969b) as well as geometry and location of bridges (Ghazvinian et al., 2007). An equivalent shear strength calculation method was developed based on the Mohr-Coulomb failure criterion, in which strength contributions from rock bridges and persistent joint areas are linearly combined (Lajtai, 1969a; Hudson and Harrison, 2000) as expressed by the following equation:

$$\tau = c_i + \sigma \cdot \tan\varphi_i = \left[K_L \cdot c_p + (1 - K_L) \cdot c_B\right] + \sigma[K_L \cdot tan_{\varphi_p} + (1 - K_L)tan_{\varphi_B}] \quad (3)$$

where τ and σ are shear strength of incipient rock joints and normal stress; c_i and $\varphi_i$are the equivalent cohesion and internal friction angle of incipient rock joints; c_p and φ_p are the cohesion and internal friction angle of persistent joint; c_B and φ_B are the cohesion and internal friction angle of intact rock bridges; K_L is the linear persistence in the direction of shearing.

This equation tends to overestimate the shear strength as it assumes that rock bridges and friction of persistent joint areas are mobilized simultaneously, that is at the same deformation (Lajtai 1969a). In addition, the Mohr-Coulomb criterion is only applicable to smooth joint surfaces; it only describes rough joints under relatively low normal stress level; Eq. (3) thus has limited usefulness in practice.

Rock bridges significantly increase the shear strength of individual incipient rock discontinuities (Shang and Zhao. 2017), especially under constant normal stiffness boundary conditions (Shang et al., 2018). They effectively produce a strength reserve and that is mobilised prior to failure occurring along the incipient joint plane (Jennings, 1970; Stimpson, 1978; Gehle and Kutter, 2003; Paolo et al., 2016). Hencher (1984) by undertaking a direct shear test on an incipient tuff joint at the core scale (54 mm in diameter) with an areal persistence of around 86% found that the rock bridge on the incipient joint plane produced a cohesion of 750 kPa. At a larger scale, a rock bridge having a size of about 150 mm X 300 mm was identified by Paolo et al. (2016) after collapse of a limestone wedge (tetrahedral block with a volume of around 28 m^3) at the Rosandra valley, north-eastern Italy. Cohesion of the bridge was back-calculated to be around 2.4 MPa (cohesion of the intact rock is 25 MPa). It is however rare to see laboratory shear testing on natural incipient rock discontinuity as it is not straightforward to secure and prepare groups of natural rock samples containing incipient discontinuities.

Numerical analysis has been used as an alternative to examine the shear strength of non-persistent rock joints, for example, using Itasca Particle Flow Code (e.g. Cundall, 1999; Park and Song, 2009; Ghazvinian et al., 2012; Shang et al., 2018) and Rock Failure Process Analysis code (e.g. Zhang et al., 2006). In numerical analysis, non-persistent rock joints containing rock bridges with different geometrical parameters are readily analysed (Shang and Zhao, 2017); the brittle failure of rock bridges often lead to a dramatic drop in shear strength (Fig. 7). Shear strength of incipient rock joints generally increases when persistence value decreases, and it also varies with spatial scale of rock bridges, as illustrated by Fig. 8 in which numerically simulated shear strength of three incipient rock joints with the same areal persistence (K=0.5) varied. Such scale dependent of strength arises from variations in the stress distribution (Rao et al., 2006) and therefore mode of fracture initiation and propagation.

4. Implications for the strength and stability of rock masses

4.1 Block size and volume for rock masses with non-persistent joint

The intersections of discontinuities in rock masses leads to discrete blocks with variable geometries (Mauldon, 1994; Kalenchuk et al., 2006), especially when discontinuities are not fully persistent. Publications accounting for discontinuity persistence and its influence on the rock block size and volume are discussed below.

Assessing rock block size and volume can be roughly categorized into three groups such as index evaluation (e.g. ISRM, 1978; Sen and Eissa, 1992), image-based measurement (e.g. Panek, 1981; Maerz, 1996), and model dissection (e.g. Goodman and Shi, 1985).

For rock masses containing several sets of persistent rock joints, rock block volume (V) within a representative rock mass can be empirically calculated by:

$$V = \frac{S_1 \cdot S_2 \cdot S_3 \cdots S_i}{sin\alpha_1 \cdot sin\alpha_2 \cdot sin\alpha_3 \cdots sin\alpha_i} \tag{4}$$

where S_i and α_i are joint spacing and angle of inclination for each joint set, respectively (Cai et al., 2004; Palmstrȍm, 2005).

Block volume calculated by Eq. (4) is an estimation of real rock block volume on the assumption that discontinuities are fully persistent. This approximation tends to be more problematic when the scale of rock mass increases (Lu and Latham, 1999). Rock bridges in fractured rock masses lead to irregular rock block shapes and larger rock block size (Longoni et al., 2012). An equivalent spacing ${S_i}'$ for incipient rock joints can be defined as (Cai and Horri, 1992):

$${S_i}' = \frac{S_i}{\sqrt[3]{K_i}} \tag{5}$$

where K_i is joint persistence for each joint set i.

Thus the equivalent rock block volume can be expressed by the following equation:

$$V = \frac{S_1 \cdot S_2 \cdot S_3 \cdots S_i}{\sqrt[3]{K_1 \cdot K_2 \cdot K_3 \cdots K_i} \cdot sin\alpha_1 \cdot sin\alpha_2 \cdot sin\alpha_3 \cdots sin\alpha_i} \tag{6}$$

It has been accepted that block size and volume are sensitive to discontinuity persistence (Rogers et al., 2007; Elmouttie and Poropat, 2012) and block volume increases when persistence decreases (Kalenchuk et al., 2006). Numerical modelling allows the sensitivity of block volume to persistence to be investigated quantitatively (Kim, 2007b; Palleske et al., 2014). Fig. 9 shows an reciprocal relationship between discontinuity persistence and rock block size (including 294 cases analysed by UDEC), and volume (including 144 cases analysed by 3DEC) with parametric analysis using the discrete element method (Kim et al., 2007b and 2007c). In Fig.9a, Groups 1-3 represent simulation cases that the standard deviation (SD) of joint angle between each joint set is 5°, and the SDs of spacing and trace length are 10, 20 and 30% of the mean values, respectively. Groups 4-6 (Fig. 9a) represent simulation cases that the standard deviation (SD) of joint angle between each joint set is 10°, and the SDs of spacing and trace length are 10, 20 and 30% of the mean values, respectively. In Fig. 9b, S represents simulation cases that the SDs of joint spacing and angle are within 30% of the mean value.

Normalised rock block size (Fig. 9a) and volume (Fig. 9b) decreased when discontinuity persistence increased, asymptotically approaching unity for fully persistent discontinuities. However it should be noted that the reciprocal relationships shown in Fig. 9 depended on the specific discontinuity orientations and number of joint sets (two sets) used in the simulation. In real projects, lithology and geological conditions should also be considered in the assessment of rock mass properties.

4.2 Mechanical properties and deformability of non-persistently jointed rock masses

4.2.1 Influence of persistence on rock mass behaviour

Many factors control the overall mechanical properties of a rock mass which include intact rock matrix strength (Hu et al., 2012a), geometrical and mechanical properties of discontinuities, discontinuity intersections (stress distribution varies with the number and arrangement of discontinuities, Mughieda, 1997) and the interactions between discontinuities and rock matrix (such as block interlocking). There have been several classic rock mass classification schemes, for example, RMR (Bieniawski 1973, 1989), Q system (Barton et al., 1975) and GSI (Hoek et al., 1995), to assess the strength of rock masses. Generally, these classification schemes are empirically developed to provide a guidance for engineering support (except for GSI, which was semi-empirically designed for rock mass strength estimation) based on engineering projects and laboratory data (Hu et al., 2012b). A specific value considering different influential factors is assessed and calculated to reflect the quality of rock masses. Nevertheless, these schemes fail to explicitly consider the influence of persistence in the mass strength determination. For example, in GSI system, discontinuity persistence is only indirectly considered by the interlocking descriptor (Cai et al., 2004); essentially discontinuities are assumed fully persistent. GSI therefore tends to underestimate the overall strength of a rock mass, especially at high confinement where interlocking effects are strong (Bharani and Kaiser 2013). Rock quality designation (RQD), originally introduced by Deere (1963) for the use in core logging, is one of the key parameters used in RMR and Q system. Sound core pieces greater than 100 mm in length are summed and expressed as a percentage of total core run. RQD however was devised to include only fully development discontinuities with zero tensile strength, so when incipient joint traces (which have considerable tensile strength) are also included in the assessment, rock mass strength is underestimated (Hencher 2014, 2015; Pells et al., 2017).

Prudencio and Van Sint Jan (2007) conducted laboratory tests on physical models of non-persistently jointed rock mass under biaxial loading condition. A set of non-persistent rock joints was made by inserting steel sheets into the mortar mixture during sample preparation. One of the key findings is that rock mass failure modes and compressive strength depended on the geometry of the discontinuity, loading stresses, and ratios of principle and intermediate stresses. Three basic failure modes were identified (i.e. failure through incipient joint plane, stepped failure and rotational failure of rock blocks).

Numerical modelling has been used to investigate the influence of persistence on overall mechanical properties of jointed rock masses. Kim et al. (2007a, b and c) examined how the incipient discontinuities with varying persistence values affect the mechanical properties of jointed rock mass. UDEC and 3DEC codes combined with experimental approaches were used in their study. Shear and compressive strengths of a jointed rock mass with and without considering persistence (represented as t, t_0, σ_c and σ_{c0} respectively, with the zero subscript indicating fully persistent case) were studied, while GSI values with and without considering persistence were calculated using the quantitative approach proposed by Cai et al. (2004). Normalised ratios found from Kim et al. (2007a, b) including t / t_0, σ_c /σ_{c0} and GSI / GSI_0 are plotted against discontinuity persistence (see Fig. 10). It can been seen that normalised shear strength (red curve) of jointed rock masses dramatically decreases when persistence increases. The analysis shows that the shear strength of rocks can be underestimated dramatically if persistence is ignored in the rock mass strength assessment. The normalised compressive strength (blue curve) and normalised GSI value (green curve) against persistence also show that the assumption of full persistence leads to strength underestimation but by a smaller extent, i.e., by about up to 1.5 times for each case.

Following their laboratory investigation of discontinuity geometry (Prudencio and Van Sint Jan 2007), the PFC3D code was used to investigate the effect of discontinuity persistence on the failure mechanism of jointed rock masses (Bahaaddini et al., 2013). Compressive strength and elastic modulus of rock masses with multiple layers of coplanar non-persistent discontinuities were examined (Fig. 11). In their study, persistence varied from 0.5 to 0.8 while other geometrical parameters were set to be constant except for the dip angle β, which varied from 0° to 90°. Their numerical results are reproduced in Fig. 12, with corresponding failure modes of samples when K=0.5 and β=90°. Compressive strength and elastic modulus of the rock mass decreased when persistence increased, for the same dip angle relative to the loading axis. Tensile cracks dominated at low persistence but decreased dramatically when persistence increased from 0.5 to 0.8 (see the insert diagrams of β=90°, Fig. 12a,). This phenomenon can be attributed to the reduction of the number of joint tips. A further investigation was reported by Bahaaddini et al. (2016); a similar methodology was used and similar results were arrived at to those plotted in Fig. 12.

4.2.2 Rock slope stability considering non-persistent discontinuities

Non-persistent rock discontinuities have significant influence on the mechanical properties and deformability of rock masses and therefore on the stability of rock engineering projects such as engineered rock slopes. Large rock volumes (compared with joint spacing) can contain many discontinuities and therefore complex stress distributions, especially where discontinuities are randomly distributed. A challenging difficulty confronting practitioners is how to consider the incipiency of discontinuities in large-scale stability analysis. In addition, the gradual development and coalescence of discontinuities over engineering time may have profound effects on stability. An illustrative example was presented by Hencher (2006), in which progressive development of sheeting joints over a period of many years was observed prior to the detachment of a large landslide in Hong Kong.

Einstein et al. (1983) proposed a probabilistic criterion for failure that was related to discontinuity data, to examine the effect of discontinuity persistence on rock slope stability. Only one set of parallel discontinuities with varying persistence was examined in their study. The "critical path" for a given discontinuity geometry (including coplanar and non-coplanar joint planes, such as en enchelon) was defined to consider strength contributions from discontinuities and intervening rock bridges as well as the spatial variability of discontinuity geometry. For this "critical path" they defined a minimum safety margin, SM, as the ratio of available resisting force to driving force. The SLOPESIM code was utilized to find the paths of minimum SM and achieve probabilistic failure analysis of a jointed rock slope. In addition, the effect of probabilistic distribution of persistence was investigated using a parametric method.

The notion of representative volume element (RVE) of jointed rock masses was proposed by Pariseau et al. (2008) aiming to simultaneously enhance the reliability of large-scale rock mass stability analysis and dramatically reduce computer run time, from hundreds of hours to several hours. The RVE of a non-persistently jointed rock mass represents the smallest volume over which a measurement can be made that will yield a value representative of the whole. In this study, the stability of engineered open pit slopes was investigated by utilizing a finite element modelling technique in which RVE were recognised for a given discontinuity geometry, rather than modelling individual discontinuities. Equivalent discontinuity properties (Pariseau et al., 2008) were calculated for a given persistence for each set of discontinuities within the RVE, and then employed in the slope stability analysis. The main contribution of RVE approach is that numerous non-persistent discontinuities within a rock mass at project scale can be effectively dealt with.

In another study of the effect of incipiency on rock mass strength behaviour, Viviana et al. (2015) proposed a method combining a probabilistic approach (assuming the distribution of the rock bridges along the sliding plane follows a fractal distribution law) using the discrete element method (DEM), to investigate translational sliding failure along a single incipient discontinuity within rock slopes. Three different sliding block geometries were investigated, that is, with block centres of gravity located in the upper part (Fig.13a), lower part (Fig.13b) and middle of sliding block (Fig.13c), respectively. For each situation, three different dip angles (30°, 50°, and 70 °) were used. The dominant slope failure mode (indicated by extent of shear versus tensile crack development) was found to be dependent on the slope geometry (dip of slope and centre of gravity) and discontinuity persistence (Fig.13). For all situations, tensile and shear cracking increased dramatically when persistence decreased which confirms the finding by Bahaaddini et al. (2013) that higher tensile cracking arises from lower discontinuity persistence. For configurations where centres of gravity were located in the upper (see the schematic diagram in Fig.13a) and middle section of the sliding block (see the schematic diagram Fig.13c), shear cracks predominate, especially for a small dip angles i.e., 30° where pure shear failure occurred. For higher dip angles, rock slopes often fail in by both tensile and shear cracking.

5. Quantification of rock discontinuity persistence

As discussed earlier, he influence of persistence on rock mass mechanical behaviour has long been known but generally has been dealt with crudely. Currently, there are no recommended methods to measure or predict discontinuity persistence. An approximation to real discontinuity size can be derived from measured trace length from rock exposures after correcting the sampling bias (e.g. Baecher et al., 1977; Priest and Hudson 1981; Mauldon 1998; Zhang et al., 2002; Latham et al., 2006) but with inherent limitations.

5.1 Discontinuity data collection and size estimation

Data acquisition of discontinuities from exposed rock faces, can be grouped into two categories: manual methods (i.e. scanline sampling and window sampling) and computer-aided methods.

5.1.1 Scanline and window sampling methods

At planar or nearly planar rock exposures, statistical sampling methods including scanline and window approaches have been widely used to measure the extent of discontinuities intersected.

In straight scanlines, a tape is laid along rock face, and the joint traces intersecting the line in a scanline survey are recorded. In practice, surveys including between 150 and 350 discontinuities are suggested and colour photos of exposed rock faces and scale makers are useful (Hudson and Priest, 1979). Scanline surveys may be grouped into two categories: quick scanline and detailed scanline. For a quick scanline survey, only the location of the scanline, the chainage of each intersection, plunge and azimuth of joint traces are recorded. Detailed scanline surveys normally also include, discontinuity types (e.g. joints, bedding, foliation, lamination and cleavage), trace length, aperture and infilling condition, planarity, waviness, termination and water condition (any evidence of seepage). A good example template of detailed scanline survey is produced by Hencher (2015), in which relative strength to parent rock was additionally suggested to be considered.

Fig. 14 diagrammatically shows a scanline survey on a planar rock face of limited extent. This survey is subject to some drawbacks, for example, sampling biases, orientation bias and censoring bias, which have been noted by many researchers (e.g. Cruden 1977). These biases are summarised as follows:

(1) Size bias. Scanlines will preferentially identify those discontinuities with a longer trace length, and small traces on exposures are missed (Priest and Hudson 1981)

(2) Orientation bias. Discontinuities striking roughly parallel to the scanline will be under-represented and excluded from the sampling results. This will lead to a serious misinterpretation of discontinuity extent as some critical information is omitted. Park and West (2002) verified and emphasised the orientation bias based on the examination of the differences in results from vertical borehole fracture mapping method and horizontal scanline sampling. Selection of

several scanline directions in the measurement of trace length can, to some extent, eliminate the orientation bias and it is recommended that scanlines should be measured in each orthogonal direction (Priest 1993; Hencher 2015)

(3) Censoring bias. Rock exposures are limited and relatively small compared with major joints. Inevitably for large discontinuities, one end or both ends, may extend beyond the visible exposure, therefore they are censored to some degree depending on discontinuity size (Cruden 1977). The censoring bias should be considered in the inference of discontinuity size (Baecher 1980).

Window sampling, another manual data acquisition technique, has also been used for sampling the discontinuities exposed at a given rock face. The preliminaries and measurement techniques are similar to scanline survey except that all discontinuities are measured in a finite area, rather than the intersection of the scanline. For setting up window sampling, a rectangle or circular area is defined on the outcrop. The window should be sufficiently large to reduce the sampling bias, with each side intersecting between 30 and 100 discontinuities. Discontinuities are counted and classified into three classes (Pahl 1981; Zhang and Einstein 2000):

(1) Discontinuities contained in the window: both ends of discontinuities are visible in the sampling domain.
(2) Discontinuities that transect the window: both ends of discontinuities are invisible in the sampling domain, this is, ends beyond the limits of window.
(3) Discontinuities that intersect the window: only one end is visible in the window and another one beyond the limits of sampling area.

Although window sampling still suffers from the censoring issue, this method normally is able to eliminate size and orientation biases (Mauldon et al., 2001). In addition, discontinuity termination characteristics can also be logged by using window sampling (Dershowitz and Einstein 1988), but it does not provide any information about discontinuity orientation or surface geometry (Priest 1993).

Manual data acquisition methods suffer from some limitations. The first is that they are labour and time consuming. In order to minimise the sampling bias, sampling should be conducted at many different locations. The operator's safety during sampling is another issue. The second is that unbiased discontinuity characterisation requires a skilled interpretation (rock engineer or geologist). The third limitation is that manual methods cannot collect data from rock exposures that are not accessible. So researchers have paid a lot attention to producing alternative ways to obtain discontinuity data from outcrop.

5.1.2 Computer aided sampling

Computer aided sampling methods for discontinuity characterisation have made significant advances over the last 25 years. An image analysis technique, perhaps the pioneer work towards this topic, was proposed by Ord and Cheung (1991) to describe discontinuities in outcrop automatically. Since then, computer-aided techniques have been developed. Roberts and Poropat (2000) proposed a digital photogrammetric technique to investigate three dimensional models of rock faces. Feng et al. (2001) proposed a portal system, in which a laser range finder was used, to identify discontinuities in outcrop. Several computer aided techniques including digital photogrammetry (e.g. Tuckey and Stead 2016), ground-based LiDAR (e.g. Mattew and Malte 2012), and digital trace mapping (Tuckey et al., 2012) have been applied to develop a standardized and adaptable methodology for assessing discontinuity persistence. An example among these techniques is shown in Fig. 15

(Tuckey et al., 2012), in which the image processing code Image-J was used to trace discontinuities and infer rock bridges. The results of the study were used to supplement field window sampling. Umili et al. (2013) developed an automatic method to map and identify discontinuity traces based on a digital surface model (DSM), which consists of a triangulated point cloud that approximates the true surface. Terrestrial Laser Scanner (TLS) and Terrestrial digital photogrammetry (TDP) have also been widely used in characterising discontinuities and rock face morphology (e.g. Rosser et al., 2005; Sturzenegger and Stead 2009 a, b; Slob 2010; Sturzenegger et al., 2011; Brideau et al., 2012). Abellan et al., (2014) comprehensively reviewed the application of TLS technique to rock exposure characterization. These methods are generally based on the segmentation of the rock exposures, and discontinuity characteristics are obtained from the boundaries and orientations of the identified planes (Umili et al., 2013). Data collected is statistically examined and is used for the rock mass characterisation.

5.1.3 Discontinuity size estimation from censored measurements

Discontinuity size is often estimated based on censored sampling measurements using the aforementioned techniques. As visible trace length does not equal to true persistence, probability distributions of trace lengths need to be corrected for sampling biases to provide an estimate of the true discontinuity size (or trace length) distribution. Well formulated probability sampling planes should be used otherwise errors will occur (Baecher and Lanney 1977). Table 1 presents a selection of key publications advancing these approaches highlighting the methods used, sampling techniques they are applicable, and major assumptions.

5.2 Discontinuity persistence in the subsurface

Geophysical techniques have been used to investigate discontinuities in the subsurface (e.g. Grandjean and Gourry 1996; Willenberg et al., 2008; Kana et al., 2013). The paper by Longoni et al. (2012) provided illustrating insights into the application of radar in the investigation of subsurface discontinuity persistence. In their work, ground penetrating radar surveys were conducted to image the 3D discontinuity planes inside rock mass, thereafter discontinuity persistence was calculated. Geological discontinuities in the subsurface are usually complex thus sometimes will frustrate geophysical sampling, geophysical approaches requires a high resolution to be able to sample discontinuities as these are relatively thin, and an experienced operator is also needed to process and interpret discontinuities within radar datasets.

5.3 Forensic excavation of rock masses

In a recent work reported by Shang et al. (2017a), a new technique, termed forensic excavation of rock masses (FERM), was introduced as an approach for investigating discontinuity areal persistence. Fig. 16 shows the FERM testing procedures. This technique involves non-explosive excavation of rock masses by injecting an expansive grout along incipient discontinuities. The agent causes the incipient rock discontinuity traces to open as open joints, thus allows the observation of areal joint surfaces and determination of areal persistence. Laboratory and field tests has been conducted on two lithologies (Midgley Grit Sandstone and Horton Formation Siltstone) by the authors, which demonstrated that FERM allows measurement of areal persistence at laboratory scale and field scale over the range of a few meters. Project scale tests will hopefully to be conducted to verify the capability of FERM at larger scales.

6. Summary, conclusion and recommendations for future research

6.1 Summary and conclusion

It has been nearly four decades since awareness of the importance of discontinuity persistence in earth science applications (Cruden 1977; ISRM 1978). Some endeavours have been made to consider persistence during the measurement of discontinuities (e.g. ISRM 1978; Priest and Hudson 1981; Latham et al., 2006) and in the assessment of rock mass stability (e.g. Einstein 1983; Pariseau et al., 2008). These endeavours however have not led to standard methods to quantify real persistence. This review has described the fundamentals of this topic e.g. definitions (incipient, mechanical discontinuities and persistence), mechanical properties of individual rock discontinuities, and those of rock masses containing non-persistent joints. State-of-the-art methodologies in the description and quantification of discontinuity persistence were summarised and reviewed.

Areal persistence, reflecting the three dimensional nature of geological discontinuities, is the best measure of persistence. Studies aiming at quantification of discontinuity persistence have been relatively few in number. In rock engineering practice, “geological judgements” are often used, but these can fail to represent the three dimensional nature of discontinuities, for example where linear persistence is used to represent areal persistence.

The size and volume of rock blocks within rock masses are sensitive to discontinuity persistence and will be underestimated if 100% persistence is assumed. Geometrical considerations based on uniform joint spacing imply a reciprocal cube-root relationship between discontinuity persistence and block size / block volume (Eq. 6), whereas previous studies using more realistic spacing distributions suggest a reciprocal relationship i.e. $V_b/V_0 \sim K^{-1}$. However, the specific lithology and geological conditions should be considered in the assessment of rock mass properties based on persistence values.

Failure modes of a rock mass are generally controlled by the discontinuities. Studies show that discontinuity persistence, orientation and number of discontinuities overshadow the efficacy of other factors. Potential for sliding failure of rock slopes along planar discontinuities is mainly controlled by the persistence and orientation of discontinuities. In addition, the spatial distributions and geometries of intact rock bridges as well as mineral infills influence the mechanical properties of incipient discontinuities (Shang et al., 2016).

6.2 Recommendations for future research

The authors recommend some topics that might be taken up for future research. These are as follows:

(1) Current definitions of persistence (i.e., Eqs. 1 and 2) only apply to planar discontinuities. Engineering applications based on the definitions will unavoidably have some limitations, as some discontinuities are not planar in shape (e.g., ‘zig-zag’ and ‘en-echelon’ fractures). Thus, there is a need to define persistence for non-planar discontinuities; thereafter a full spectrum of discontinuity persistence is able to be quantified and implemented into engineering applications such as discrete fracture network modelling.

(2) Up to date, rock engineering practise lacks standard methods to deal with the incipiency of some discontinuities, i.e. those that are not fully developed mechanical break with some tensile strength. The degree of incipiency of discontinuities can be described by their tensile strengths relative to that of parent rock. Tensile strength is

suggested because incipient discontinuity shear strength is complicated by other factors, including roughness and asperities of the persistent sections. A classification scheme differentiating incipiency of discontinuities has been conceptually proposed by Hencher (2014) with different bands including open fracture, weak, moderate and high. Direct tensile tests on incipient rock discontinuities have been conducted by Shang (2016) in the laboratory to follow up that topic. However, limited tests were involved due to the difficulty of the natural sample collection and preparation. It is therefore suggested that more tests need to be performed to facilitate the production of the classification scheme of discontinuity incipiency.

(3) In a recent study by Shang et al. (2017a), the quantification of areal persistence was attempted by “forensic excavation of rock masses (at block sale)”; this technique needs proof of concept at larger scales.

(4) Non-invasive quantification of persistence might also be achieved using geophysics, which if successful will improve the ability to predict rock mass properties.

Acknowledgments The authors thank the editor-in-chief Dr. Janusz Wasowski and three anonymous reviewers for their valuable comments.

References

Abellan, A., Oppikofer, T., Jahoyedoff, M., Rosser, N.J., Lim, M., Lato, M.J., 2014. Terrestrial laser scanning of rock slope instabilities. Earth Surf. Process. Landf. 39, 80-97.

Baecher, G.B., 1980. Progressively censored sampling of rock joints traces. Math. Geo. 12(1), 33-40.

Baecher, G.B., Lanney, N.A., Einstein, H.H., 1978. Statistical description of rock properties and sampling. In: Proceeding of the 18th U.S. Symposium on Rock Mechanics, Colorado, pp. 22-24.

Bahaaddini, M., Sharrock, G., Hebblewhite, B.K., 2013. Numerical investigation of the effect of joint geometrical parameters on the mechanical properties of a non-persistent jointed rock mass under uniaxial compression. Comput. Geotech. 49, 206-225.

Bahaaddini, M., Hagan, P., Mitra, R., Hebblewhite, B.K., 2016. Numerical study of the mechanical behaviour of nonpersistent jointed rock masses. Int. J. Geomech. 16(1),1-10.

Barton, N., 1976. The shear strength of rock and rock joints. Int. J. Rock Mech. Min. Sci. 13, 255-279.

Bharani, N., and Kaiser, P.K., 2013. Strength degradation of non-persistently jointed rock mass. Int. J. Rock Mech. Min. Sci. 62, 28-33.

Bieniawski, Z.T., 1973. Engineering classification of jointed rock masses. Trans. S. Afr. Inst. Civ. Eng. 15, 335-344.

Bieniawski, Z.T., 1989. Engineering Rock Mass Classifications. Wiley, New York, pp. 249.

Borrelli, L., Greco, R., Gulla, G., 2007. Weathering grade of rock masses as a predisposing factor to slope instabilities: reconnaissance and control procedures. Geomorphology. 87, 158-175.

Brian, D.C., Greg, M.S., 2016. Rockfall triggering by cyclic thermal stressing of exfoliation fractures. Nat. Geosci. 9, 395-400.

Brideau, M.A., Sturzenegger, M., Stead, D., Jaboyedoff, M., Lawrence, M., Roberts, N., Ward, B., Millard, T., Clague, J., 2012. Stability analysis of the 2007

Chehalis lake landslide based on long-range terrestrial photogrammetry and airborne LiDAR data. Landslides. 9, 75-91.

Bridges, M.C., 1976. Presentation of fracture data for rock mechanics. In: Proceeding of 2nd Australian – New Zealand Conference on Geomechanics, pp. 144-148.

Cai, M., Horri, H., 1992. A constitutive model of highly jointed rock masses. Mech. Mater. 13(3), 217-246.

Cai, M., Kaiser, P.K., Uno, H., Tasaka, Y., Minami, M., 2004. Estimation of rock mass deformation modulus and strength of jointed hard rock masses using the GSI system. Int. J. Rock Mech. Min. Sci. 41, 3-19.

Cravero, M., Labichino, G., 2004. Analysis of the flexural failure of an overhanging rock slab. Int. J. Rock Mech. Min. Sci. 41(S1), 605-610.

Cruden, D.M., 1977. Describing the size of discontinuities. Int. J. Rock Mech. Min. Sci.144, 133-137.

Cundall, P.A., 1999. Numerical experiments on rough joints in shear using a bonded particle model. In: Aspects of tectonic faulting. Berlin, Springer, pp. 1-9.

Deere, D.U., 1963. Technical description of rock cores for engineering purposes. In: 13th Colloquium, International Society for Rock Mechanics, Salzburg, Austria, pp. 16-22.

Deparis, J., Johgmans, D., Garambois, S., Levy, C., Baillet, L., Meric O., 2011. Geophysical detection and structural characterization of discontinuities in rock slopes. Rockfall Engineering, Wiley, ISTE, pp. 1-38.

Dershowitz, W.S., Einstein, H.H., 1988. Characterizing rock joint geometry with joint system models. Rock Mech. Rock Eng. 21, 21-51.

Einstein, H.H., Veneziano, D., Baecher, G.B., Oreilly, K.J., 1983. The effect of discontinuity persistence on rock slope stability. Int. J. Rock Mech. Min. Sci. 20(5), 227-236.

Elmouttie, M.K., Poropat, G.V., 2012. A method to estimate in situ block size distribution. Rock Mech. Rock Eng. 45, 401-407.

Feng, Q., Sjogren, P., Stephansson, O., Jing, L., 2001. Measuring fracture orientation at exposed rock faces by using a non-reflector total station. Eng. Geol. 59(1-2), 133-146.

Gehle, C., Kutter, H.K., 2003. Breakage and shear behaviour of intermittent rock joints. Int. J. Rock Mech. Min. Sci. 30(40), 687-700.

Ghazvinian, A., Nikudel, M.R., Sarfarazi, V., 2007. Effect of rock bridge continuity and area on shear behaviour of joints. In: 11th Congress of the International Society for Rock Mechanics, pp. 247-250.

Ghazvinian, A., Sarfarzai, V., Schubert, W., 2012. A study of the failure mechanism of planar non-persistenct open joints using PFC2D. Rock Mech. Rock Eng. 45, 677-693.

Goodman, R.E., Shi, G., 1985. Block theory and its application to rock engineering, Prentice-Hall, New Jersey, p. 352

Goudie, A.S., 2016. Quantification of rock control in geomorphology. Earth-Sci. Rev. 159, 374-387.

Grandjean, G., Gourry, J.C., 1996. GPR data processing for 3D fracture mapping in a marble quarry. J. Appl. Geophys. 36, 19-30.

Heike, W., Simon, L., Erik, E., Keith, F.E., Thomas, S., Bjorn, H., Hansruedi, M., Alan, G.G., 2008. Internal structure and deformation of an unstable crystalline rock mass above Randa (Swithzerland): Part I – Internal structure from integrated geological and geophysical investigations. Eng. Geol. 101, 1-14.

Hencher, S.R., 2006. Weathering and erosion process in rock - implications for geotechnical engineering. In: Proceedings symposium on Hong Kong soils and rocks, Centre for research and progessional development, IMMM, Geological Society, HKRG, Hong Kong, pp. 29-79.

Hencher, S.R., 2014. Characterizing discontinuities in naturally fractured outcrop analogues and rock core: the need to consider fracture development over geological time. Advances in the study of fractured reservoirs. Geol. Soc. London Spec. Publ. 374, 113-123.

Hencher, S.R., 2015. Practical rock mechanics. Taylor and Francis Group, London, pp.356.

Hencher, S.R., 1984. Three direct shear tests on volcanic rock joints. Geotechnical Control Office Information Notes, IN 15/84. Hong Kong Governments, pp. 33 (unpublished).

Hoek, E., Kaiser, P.K., Bawden, W.F., 1995. Support of underground excavations in hard rock. Rotterdam, Balkema, p. 215.

Hu, J., Shang, J., Tao, L., 2012a. Rock mass quality evaluation of underground engineering based on RS-TOPSIS method. J. Cent. South Univ. 43(11), 4412-4419.

Hu, J., Xu, H., Luo, X., Shang, J., Ruan, D., 2012b. Determination of mechanical parameters of fractured rock mass based on GSI. J. Guangxi Univ. 37(1), 178-183.

Hudson, J.A., Harrison, J.P., 2000. Engineering rock mechanics: An interdiction to the principles. Pergamon, p. 441.

Hudson, J.A., Priest, S.D., 1979. Discontinuities and rock mass geometry. Int. J. Rock Mech. Min. Sci.16, 339-362.

ISRM, 1978. Suggested methods for the quantitative description of discontinuities in rock masses. Int. J. Rock Mech. Min. Sci. 15, 319-368.

Jennings, J.E., 1970. A mathematical theory for the calculation of the stability of slopes in open cast mines: Planning Open Pit Mines. In: Proceedings of the Symposium on the Theoretical Background to the Planning of Open Pit Mines with Special Reference to Slope Stability, Johannesburg, pp. 87-102.

Jiang, M.J., Jiang, T., Crosta, G.B., Shi, Z.M., Chen, H., Zhang, N., 2015. Modelling failure of jointed rock slope with two main joint sets using a novel DEM bond contact model. Eng. Geol. 193, 79-96.

Jimenze-Rodriguez, R., Sitar, N., 2006. Inference of discontinuity trace length distributions using statistical graphical models. Int. J. Rock Mech. Min. Sci. 43, 877-893.

Kalenchuk, K.S., Diederichs, M.S., Mckinnon, S., 2006. Characterizing block geometry in jointed rock masses. Int. J. Rock Mech. Min. Sci. 43(8): 1212-1225.

Kana AA; West LJ; Clark RA (2013) Fracture aperture and fill characterization in a limestone quarry using GPR thin-layer AVA analysis, Near Surface Geophysics, 11, 293-305.

Kevin, J.O., 1980. The effect of joint plane persistence on rock slope reliability. Ph.D. thesis, Massachusetts Institute of Technology, United State, p. 553.

Kim, B.H., Cai, M., Kaiser, P.K., 2007a. Rock mass strength with non-persistent joints. In: 1st Canada – U.S. Rock Mechanics Symposium, Vancouver, Canada, pp. 1-8.

Kim, B.H., Cai, M., Kaiser, P.K., Yang, H.S., 2007b. Estimation of block sizes for rock masses with non-persistent joints. Rock Mech. Rock Eng. 40, 169-192.

Kim, B.H., Kaiser, P.K., Grasselli, G., 2007c. Influence of persistence on behaviour of fractured rock masses. Rock physics and geomechanics in the study of reservoirs and repositories. Geol. Soc. London Spec. Publ. 284, 161-173.

Kulatilake, P.H.S.W., Wu, T.H., 1984. Estimation of mean trace length of discontinuities. Rock Mech. Rock Eng. 17, 215-232.

Lajtai, E.Z., 1969a. Shear strength of weakness planes in rock. Int. J. Rock Mech. Min. Sci. 6, 499-515.

Lajtai, E.Z., 1969b. Strength of discontinuous rocks in direct shear. Geotechnique. 19(2), 218-233.

Latham, J.P., Meulen, J.V., Dupray, S., 2006. Prediction of in-situ block size distributions with reference to armourstone for breakwaters. Eng. Geol. 86, 19-36.

Li, X., Zuo, Y., Zhuang, X., Zhu, H., 2014. Estimation of fracture trace length distributions using probability weighted moments and L-moments. Eng. Geol. 168, 69-85.

Longoni, L., Arosio, D., Scaioni, M., Papini, M., Zanzi, L., Roncella, R., Brambilla, D., 2012. Surface and subsurface non-invasive investigations to improve the characterization of a fractured rock mass. J. Geophys. Eng. 9, 461-472.

Lu, P., Latham, J.P., 1999. Developments in the assessment of in-situ block size distributions of rock masses. Rock Mech. Rock Eng. 32(1), 29-49.

Lyman, G.J., 2003. Rock fracture mean trace length estimation and confidence interval calculation using maximum likelihood methods. Int. J. Rock Mech. Min. Sci. 40, 825-832.

Maerz, H.H., 1996. Image sampling techniques and requirements for automated image analysis of rock fragmentation. In: Proceedings of the FRAGBLAST 5 Workshop on Measurement of Blast Fragmentation, Montreal, Quebec, Canada, pp. 115-120.

Mattew, J.L., Malte, V., 2012. Automated mapping of rock discontinuities in 3D lidar and photogrammetry models. Int. J. Rock Mech. Min. Sci. 54, 150-158.

Mauldon, M., 1994. Intersection Probabilities of impersistent joints. Int. J. Rock Mech. Min. Sci. 31(2), 107-115.

Mauldon, M., 1998. Estimating mean fracture trace length and density from observations in convex windows. Rock Mech. Rock Eng. 31(4), 201-216.

Mauldon, M., Dunne, W.M., Rohrbaugh Jr, M.B., 2001. Circular scanlines and circular windows: new tools for characterizing the geometry of fracture traces. J. Struct. Geol. 23, 247-258.

Mughieda, O., 1997. Failure mechanisms and strength of non-persistent rock joints. Ph.D. thesis, University of Illinois at Urbana-Champaign, United State, p. 512.

Norbury, D., 2010. Soil and rock description in engineering practice. CRC Press, Taylor & Francis Group, USA, p. 288.

Odling, N.E., Gillespie, P., Bourgine, B., Castaing, C., Chiles, J.P., Christensen, N.P., Fillion, E., Genter, A., Olsen, C., Thrane, L., Trice, R., Aarseth, E., Walsh, J.J., Watterson, J., 1999. Variations in fracture system geometry and their implications for fluid flow in fractured hydrocarbon reservoirs. Petrol. Geosci. 5, 373-384

Ord, A., Cheung, L.C., Hobbs, B.E., Blanc, D.L., 1991. Automatic mapping of rock exposures for geotechnical purposes. In: The 2nd Australian Conference on

Computer Applications in the Mineral Industry, The University of Wollongong, Australia, pp. 1-6.
Pahl, P.J., 1981. Estimating the mean length of discontinuity traces. Int. J. Rock Mech. Min. Sci. 18(3), 221-228.
Palleske, C., Diederichs, M.S., Hutchinson, D.J., Elimo, D., 2014. Block size distributions as a rock mass classification tool. In: 48th U.S. Rock Mechanics/Geomechanics Symposium, Minneapolis, Minnesota, pp. 1-8.
Palmstròm, A., 2005. Measurements and correlations between block size and rock quality designation (RQD). Int. J. Rock Mech. Min. Sci. 20, 362-377.
Panek, L.A., 1981. Design and operation of caving and sublevel stopping mines. Society for Mining Metallurgy, p. 843.
Paolo, P., Alberto, A., and Elia R., 2016. 3D stress-strain analysis of a failed limestone wedge influenced by an intact rock bridge. Rock Mech. Rock Eng. 49, 3223-3242.
Pariseau, W.G., Puri, S., and Schmelter, S.C., 2008. A new model for effects of impersistent joint sets on rock slope stability. Int. J. Rock Mech. Min. Sci. 45, 122-131.
Park, H.J., West, T.R., 2002. Sampling bias of discontinuity orientation caused by linear sampling technique. Eng. Geol. 66, 99-110.
Park, J.W., Song, J.J., 2009. Numerical simulation of a direct shear test on a rock joint using a bounded-particle model. Int. J. Rock Mech. Min. Sci. 46, 1315-1328.
Paronuzzi, P., Serafini, W., 2009. Stress state analysis of a collapsed overhanging rock slab: A case study. Eng. Geol. 108: 65-75.

Pells, P., Bieniawski, Z.T.R., Hencher, S.R., Pells, S., 2017. Rock quality designation (RQD): Time to rest in peace. Can. Geotech. J. 54: 825-834.

Piggott, A.R., Elsworth, D., 1992. Analytical models for flow through obstructed domains. J. Geophys. Res. 97(B2), 2085-2092.

Priest, S.D., 1993. Discontinuity analysis for rock engineering. Chapman & Hall, London, p. 473.

Priest, S.D., and Hudson, J.A., 1981. Estimation of discontinuity spacing and trace length using scanline surveys. Int. J. Rock Mech. Min. Sci.18, 183-197.

Prudencio, M., Van Sint Jan, M., 2007. Strength and failure modes of rock mass models with non-persistent joints. Int. J. Rock Mech. Min. Sci. 44, 890-902.

Rao, Q., Sun, Z., Stephansson, O., Li, C. Stillborg, B., 2003. Shear fracture (Mode II) of brittle rock. Int. J. Rock Mech. Min. Sci. 40, 355-375.

Rawnsley, K.D., 1990. The influence of joint origin on engineering properties. Ph.D. thesis, the University of Leeds, Leeds, United Kingdom, p.388.

Roberts, G., Poropat, G.V., 2000. Highwall joint mapping in 3-D at the Moura mine using SIROJOINT. In: Bowen Basin Symposium, Coal and Mining The New Millennium, Rockhampton, pp. 371-377.

Robertson, A.M., 1970. The interpretation of geological factors for use in slope theory. In: Planning Open Pit Mines. Van Rensburg, P.W.J. (Ed.). Cape Town, South Africa: Balkema, pp. 55-71.

Rogers, S.F., Kennard, D.K., Dershowitz, W.S., Van As, 2007. Characterising the in situ fragmentation of a fractured rock mass using a discrete fracture network approach. In: 1st Canada – US. Rock Mechanics Symposium, pp. 137-144.

Rosser, N.J., Petley, D.N., Lim, M., Dunning, S.A., Allison, R.J., 2005. Terrestrial laser scanning for monitoring the process of hard rock coastal cliff erosion. Q. J. Eng. Geol. Hydroge. 38(4), 363-375.

Sen. Z., Eissa, E.A., 1992. Rock quality charts for log-normally distributed block sizes. Int. J. Rock Mech. Min. Sci. 29(1), 1-12.

Shang, J., Hu, J., Zhou, K., 2013. Numerical tests on heterogeneous effect in damage and acoustic emission characteristic of rocks under uniaxial loading. J. Cent. South Univ. 6, 2470-2475.

Shang, J., Hencher, S.R., West, L.J., 2015. Tensile strength of incipient rock discontinuities, In: Proceedings of the ISRM regional sysposium Eurock 2015 & 64th Geomechanics Colloquium, Salzburg, Austria, pp. 565-570.

Shang, J., 2016. Persistence and tensile strength of incipient rock discontinuities. Ph.D. thesis, University of Leeds, United Kingdom, p. 248.

Shang, J., Hencher, S.R., West, L.J., 2016. Tensile strength of geological discontinuities including bedding, rock joints and mineral veins. Rock Mech. Rock Eng. 49(11), 4213-4225.

Shang, J., Hencher, S.R., West, L.J., Handley, K., 2017a. Forensic excavation of rock masses: a technique to investigate discontinuity persistence. Rock Mech. Rock Eng. 50(11), 2911-2928.

Shang, J., Duan, K., Gui, Y., Handley, K. Zhao, Z., 2017b. Numerical investigation of the direct tensile behaviour of laminated and transversely isotropic rocks containing incipient bedding planes with different strengths. Comput. Geotech. https://doi.org/10.1016/j.compgeo.2017.11.007.

Shang, J., West, L.J., Hencher, S.R., Zhao, Z., 2017c. Tensile strength of large-scale incipient rock joints: a laboratory investigation. Acta Geotech. https://doi.org/10.1007/s11440-017-0620-7

Shang, J., Zhao, Z., 2017. 3D particle-based DEM investigation into the shear behaviour of incipient rock joints with various geometries of rock bridges. Rock Mech. Rock Eng. Under Review.

Shang, J., Zhao, Z., Ma, S., 2018. On the shear failure of incipient rock discontinuities under CNL and CNS boundary conditions: Insights from DEM modelling. Eng. Geol. 234(21): 153-166.

Slob, S., 2010. Automated rock mass characterisation using 3-D terrestrial laser scanning. Ph.D. thesis, The University of Twente, Netherlands, p.301.

Song, J.J., Lee, C.I., 2001. Estimation of joint length distribution using window sampling. Int. J. Rock Mech. Min. Sci. 38, 519-528.

Stimpson, B., 1978. Failure of slopes containing discontinuous planar joints. In: Proceedings of the 19th US Symposium on Rock Mechanics, Stateline, Nevada, pp. 296-302.

Sturzenegger, M., Stead, D., 2009a. Quantifying discontinuity orientation and persistence on high mountain rock slopes and large landslides using terrestrial remote sensing techniques. Nat. Hazards Earth Syst. Sci. 9, 267-287.

Sturzenegger, M., Stead, D., 2009b. Close-range terrestrial digital photogrammetry and terrestrial laser scanning for discontinuity characterization on rock cuts. Eng. Geol. 106(3-4), 163-182.

Sturzenegger, M., Stead, D., Elmo, D., 2011. Terrestrial remote sensing-based estimation of mean trace length, trace intensity and block size/shape. Eng. Geol. 119(3-4), 96-111.

Tating, F., Hack, R., Jetten, V., 2013. Engineering aspects and time effects of rapid deterioration of sandstone in the tropical environment of Sabah, Malaysia. Eng. Geol. 159, 20-30.

Tuckey, Z., Stead, D., 2016. Improvements to field and remote sensing methods for mapping discontinuity persistence and intact rock bridges in rock slopes. Eng. Geol. 208, 136-153.

Tuckey, Z., Stead, D., Sturzenegger, M., Elmo, D., Terbrugge, P., 2012. Towards a methodology for characterizing intact rock bridges in large open pits: In: 46th US Rock Mechanics/Geomechanics Symposium held in Chicago, IL, USA, pp. 24-27.

Umili, G., Ferrero, A., Einstein, H.H., 2013. A new method for automatic discontinuity traces sampling on rock mass 3D model. Comput. Geosci. 51,182-192.

Viviana, B.S., Luc, S., Frederic-Victor, D., Marc, E., 2015. DEM analysis of rock bridges and the contribution to rock slope stability in the case of translational sliding failures. Int. J. Rock Mech. Min. Sci. 80, 67-78.

Wang, X.G., Jia, Z.X., Chen, Z.Y., Xu, Y., 2016. Determination of discontinuity persistent ratio by Monte-Carlo simulation and dynamic programming. Eng. Geol. 203, 83-98.

Wasantha, P.L.P., Ranjith, P.G., Xu, T., Zhao, J., Yan, Y.L., 2014. A new parameter to describe the persistency of non-persistent joints. Eng. Geol.181, 71-77.

Wieczorek, G.F., Jager, S., 1996. Triggering mechanisms and depositional rates of postglacial slope-movement processes in the Yosemite Valley, California. Geomorphology. 15, 17-31.

Willenberg, H., Simon, L., Eberhardt, E., Evans, K.F., Spillmann, T., Heincke, B., Maurer, H., Green, A.G., 2008. Internal structure and deformation of an unstable crystalline rock mass above Randa (Switzerland): Part I – Internal structure from integrated geological and geophysical investigations. Eng. Geol.101, 1-14.

Zhang, H.Q., Zhao, Z.Y., Tang, C.A., Song, L, 2006. Numerical study of shear behaviour of intermittent rock joints with different geometrical parameters. Int. J. Rock Mech. Min. Sci. 43, 802-816.

Zhang, L., Einstein, H.H., 2000. The planar shape of rock joints. Rock Mech. Rock Eng. 43(1), 55-68.

Zhang, L., Einstein, H.H., Dershowitz, W.S., 2002. Stereological relationship between trace length and size distribution of elliptical discontinuities. Geotechnique. 52(6), 419-433.

Zheng, Y., Xia, L., Yu, Q.C., 2015. Analysis of the removability and stability of rock blocks by considering the rock bridge effect. Can. Geotech. J. 53(3), 384-395.

Zimmerman, R.W., Chen, D.W., Cook, N.G.W., 1992. The effect of contact area on the permeability of fractures. J. Hydrol. 139, 79-96.

Figure Captions

Fig 1 Partially developed discontinuities that are incipient (non-persistent), Horton-in-Ribbesdale, Yorkshire, England.

Fig 2 a Section of andesitic tuff cores (Hong Kong) with incipient and mechanical discontinuities and **b** Same core (disassembled). Relative tensile strength, i.e., high, moderate and weak strength relative to the strength of the parent rock, is proposed to differentiate these discontinuities. Adapted from Hencher (2014).

Fig 3 A Face cut by a diamond wire saw in dimension stone quarry in granite near Tui, Galicia, Spain. Joints 1 and 2 are in earlier incipient stages (which are always poorly defined by current standards). Joint 3 is in later incipient stage and it has a persistent area partially, allowing seepage of fluid. After Shang et al. (2016)

Fig 4 Definitions of rock discontinuity persistence. **a** Areal extent of a discontinuity plane (true persistence) and **b** Linear extent definition (approximation of persistence).

Fig 5 Slope with daylighting rock slabs threatening highway in central Taiwan. The incipient nature of the discontinuities contributes tensile and shear strength and allows temporary stability.

Fig 6 General view of a collapsed overhanging limestone slab located at northern part of Cellina Valley gorge on January 26th, 1999. A rock bridge (red-hatched area) was exposed after failure. The average tensile strength of this rock bridge was calculated as 5.19 MPa through back-analysis. After Paronuzzi and Serafini (2009).

Fig 7 Relationship between shear displacement and horizontal shear force for various numerical models containing non-persistent rock joint with different geometrical parameters. Adapted from Zhang (2006).

Fig 8 Stress and strain curves of Midgley Grit Sandstone joints with the same areal persistence (K=0.5) in numerical direct shear tests under constant normal stresses of 4 and 6 MPa. Three samples showing the spatial distribution of rock bridges (Rb) and persistent joints (Pj) are shown. Particles representing rock matrix (within the top and bottom shear boxes) are not shown for clarity. After Shang and Zhao (2017).

Fig 9 Relationship between joint persistence and normalized block size (**a**) and block volume (**b**). Raw data from Kim et al. (2007b and 2007c).

Fig 10 Relationship between relative rock mass strengths and persistence. Raw data from Kim et al. (2007b and 2007b).

Fig 11 Discontinuity geometrical parameters used in the numerical modelling by Bahaaddini et al. (2013). Reproduced from Bahaaddini et al. (2013).

Fig 12 Effects of discontinuity persistence on relative compressive strength of rock masses (**a**) and on relative elastic modulus of rock masses (**b**). Note that yellow is rock matrix in PFC model; green is non-persistent rock joint; red is tension crack and blue is shear crack (rarely can be seen). K refers to linear persistence. Adapted from Bahaaddini et al. (2013).

Fig 13 DEM study results of the relationship between number of micro-cracks and discontinuity areal persistence. Schematic diagrams of simulated slopes with three different geometries are included (cracks are not shown): Centres of gravity were located in the upper part (**a**), lower part (**b**) and the middle (**c**), respectively. Shear cracks dominated when centres of gravity were located in the upper part (**a**) and middle (**c**) of sliding block. Both tensile and shear cracks occurred when centre of gravity was in the lower part of block. The dashed lines correspond to tensile crack while continuous lines represent shear crack. Adapted from Viviana et al. (2015)

Fig 14 Diagrammatic representation of discontinuity traces intersecting a scanline set up on a planar exposure of limited extent. For small size discontinuities or those that are roughly parallel to scanline or concealed, bias will occur when sampling. Adapted from Latham et al. (2006).

Fig 15 a Digital trace mapping of incipient discontinuities and blast-induced fractures on local part of the Stawamus Chief (granite), British Columbia, Canada; **b** Discontinuity traces were analysed after tracing. Irregular blast-induced fractures were traced in red, bedding planes traced in green and scattered joints traced in cyan and orange. After Tuckey et al. (2012).

Fig 16 Schematic diagram showing the testing procedures for the forensic excavation of rock masses (FERM). After Shang et al. 2017a

Fig 1

954 .

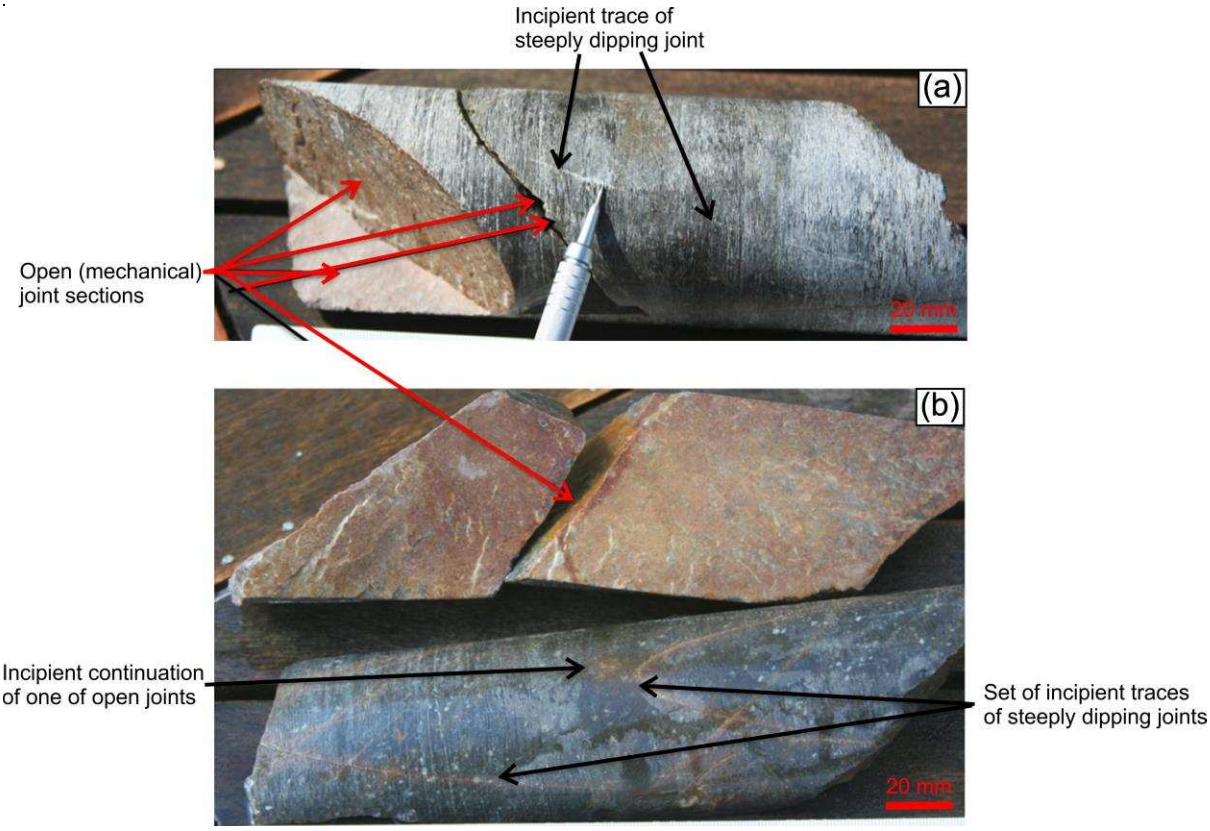

955

956 Fig 2

957

958

Fig 3

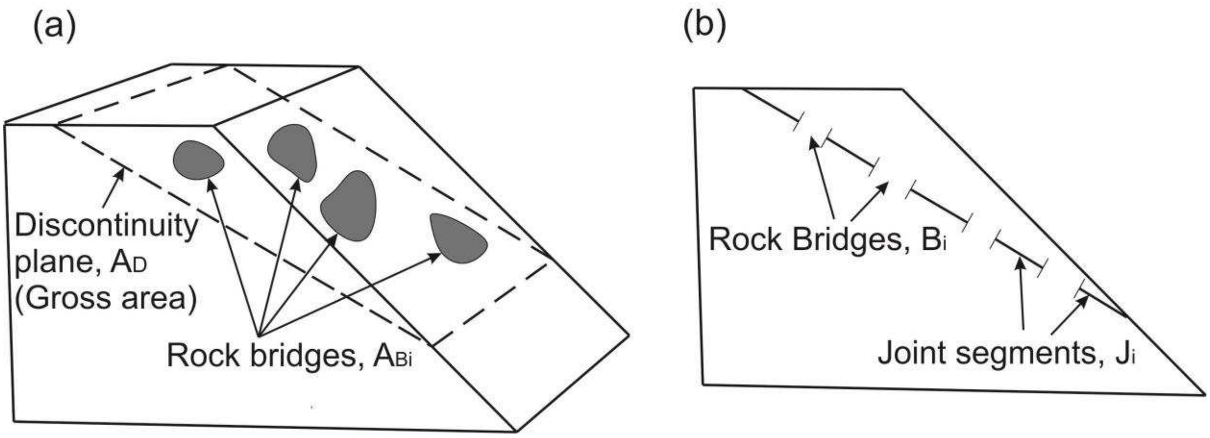
(a)
Discontinuity plane, AD (Gross area)
Rock bridges, ABi
(b)
Rock Bridges, Bi
Joint segments, Ji

Fig 4

Fig 5

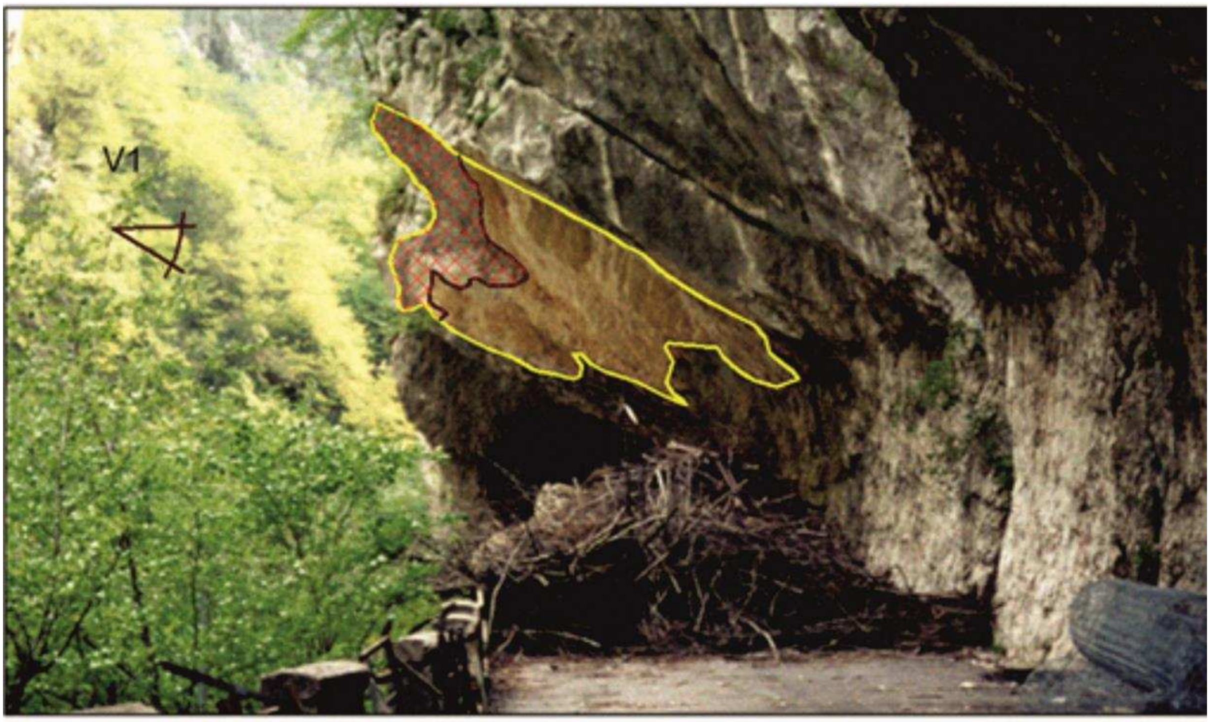

Fig 6

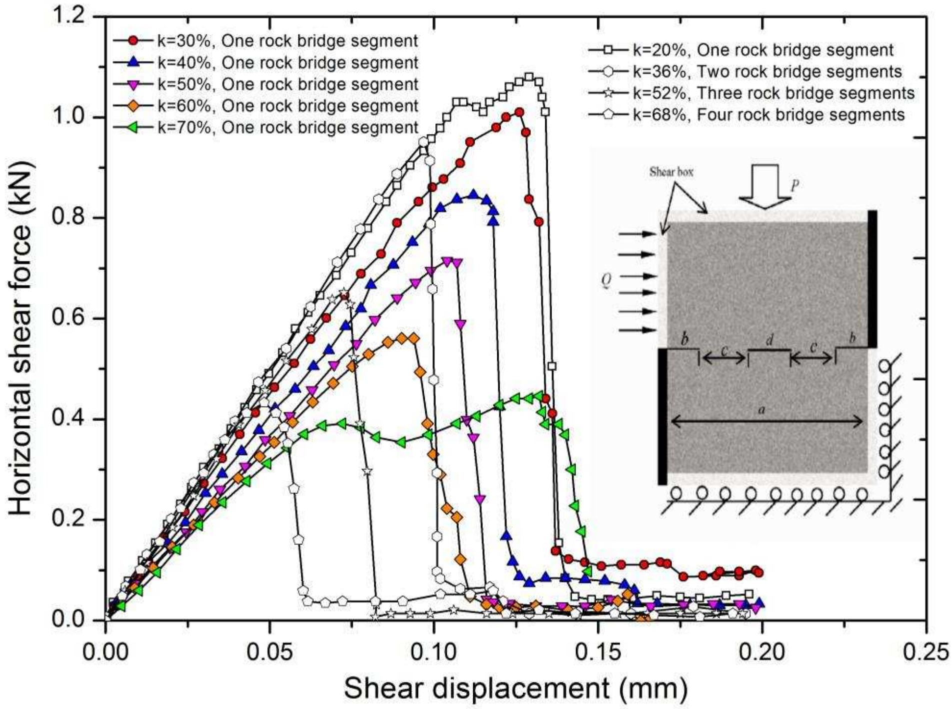

k=30%, One rock bridge segment
k=40%, One rock bridge segment
k=50%, One rock bridge segment
k=60%, One rock bridge segment
k=70%, One rock bridge segment
k=20%, One rock bridge segment
k=36%, Two rock bridge segments
k=52%, Three rock bridge segments
k=68%, Four rock bridge segments
Shear box
P
Q
b
c
d
c
b
a
Horizontal shear force (kN)
Shear displacement (mm)
0.0
0.2
0.4
0.6
0.8
1.0
1.2
0.00
0.05
0.10
0.15
0.20
0.25

Fig 7

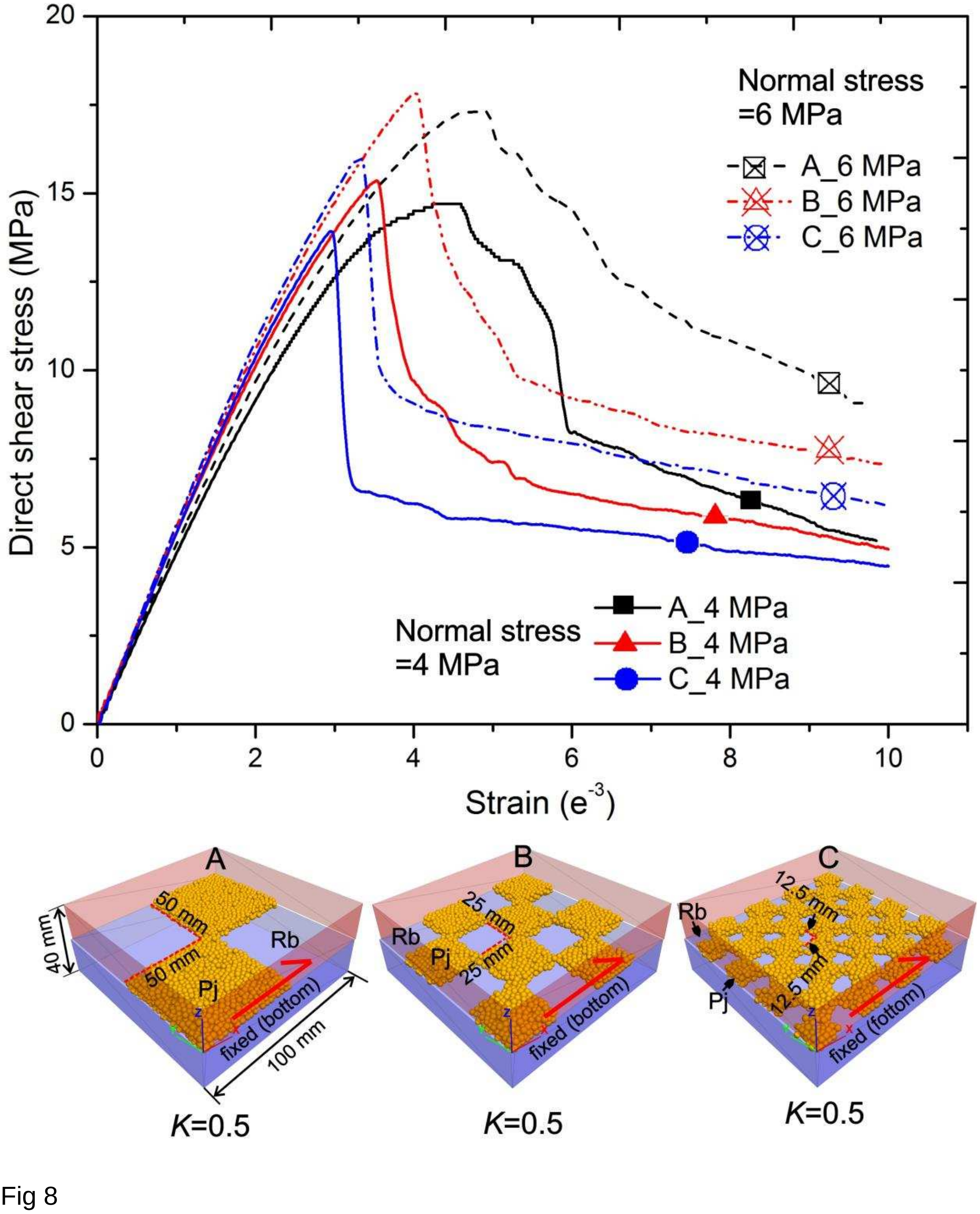

Normal stress
=6 MPa
A_6 MPa
B_6 MPa
C_6 MPa
Normal stress
=4 MPa
A_4 MPa
B_4 MPa
C_4 MPa
Direct shear stress (MPa)
Strain (e^{-3})
0
5
10
15
20
0
2
4
6
8
10
A
B
C
50 mm
50 mm
40 mm
100 mm
Rb
Pj
fixed (bottom)
25 mm
25 mm
12.5 mm
12.5 mm
fixed (fottom)
K=0.5
K=0.5
K=0.5

Fig 8

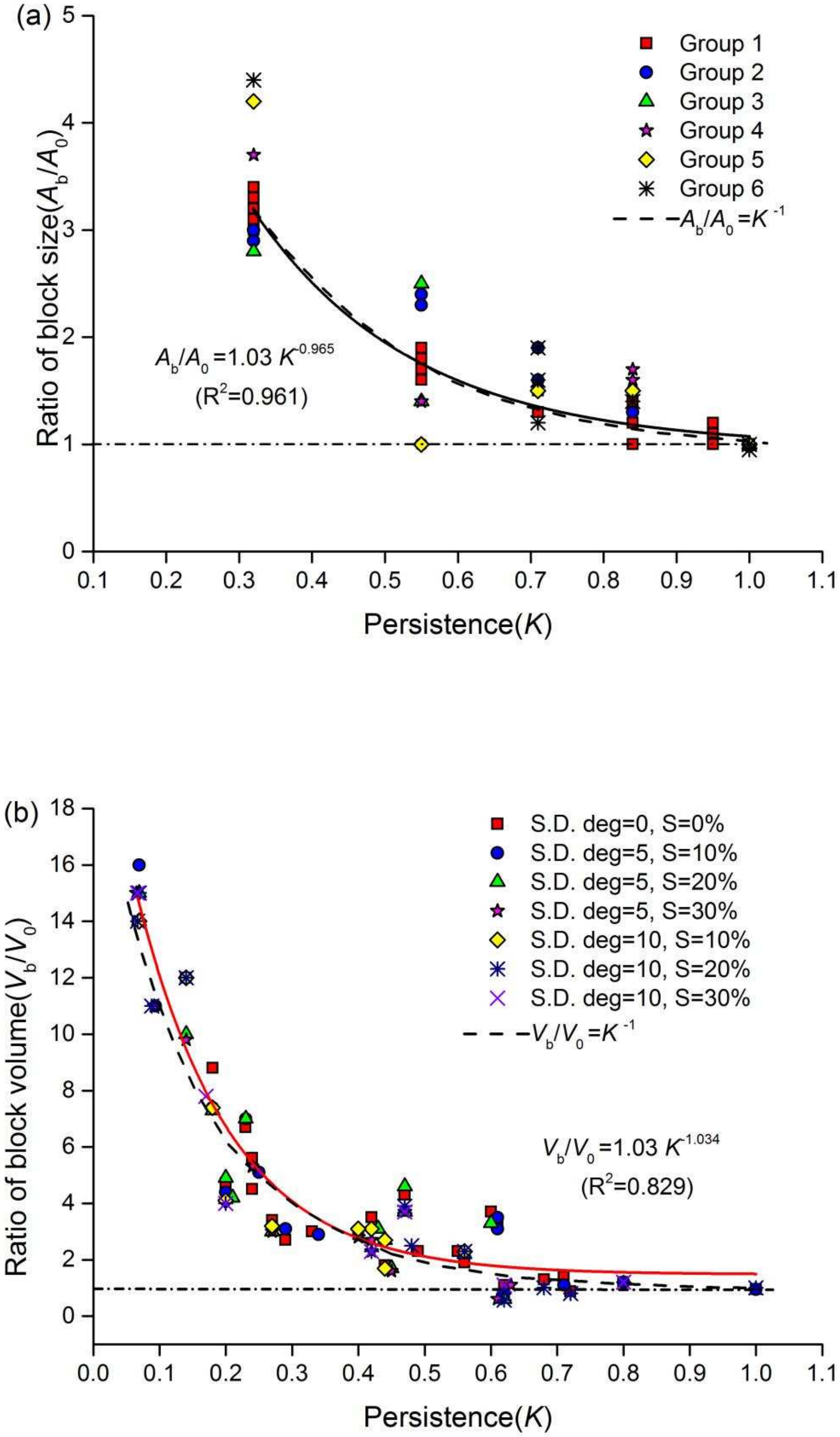
(a)
Ratio of block size(A_b/A_0)
Persistence(K)
Group 1
Group 2
Group 3
Group 4
Group 5
Group 6
$A_b/A_0=K^{-1}$
$A_b/A_0=1.03\ K^{-0.965}$
(R^2=0.961)
(b)
Ratio of block volume(V_b/V_0)
Persistence(K)
S.D. deg=0, S=0%
S.D. deg=5, S=10%
S.D. deg=5, S=20%
S.D. deg=5, S=30%
S.D. deg=10, S=10%
S.D. deg=10, S=20%
S.D. deg=10, S=30%
$V_b/V_0=K^{-1}$
$V_b/V_0=1.03\ K^{-1.034}$
(R^2=0.829)

Fig 9

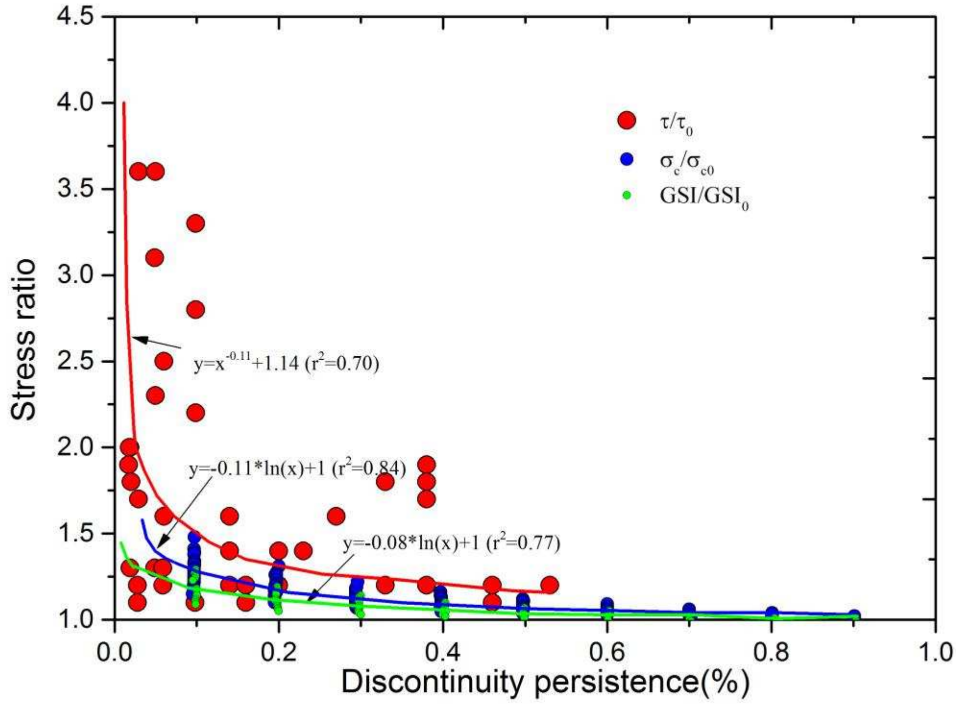

Stress ratio
Discontinuity persistence(%)
τ/τ0
σc/σc0
GSI/GSI0
y=x^-0.11+1.14 (r²=0.70)
y=-0.11*ln(x)+1 (r²=0.84)
y=-0.08*ln(x)+1 (r²=0.77)

Fig 10

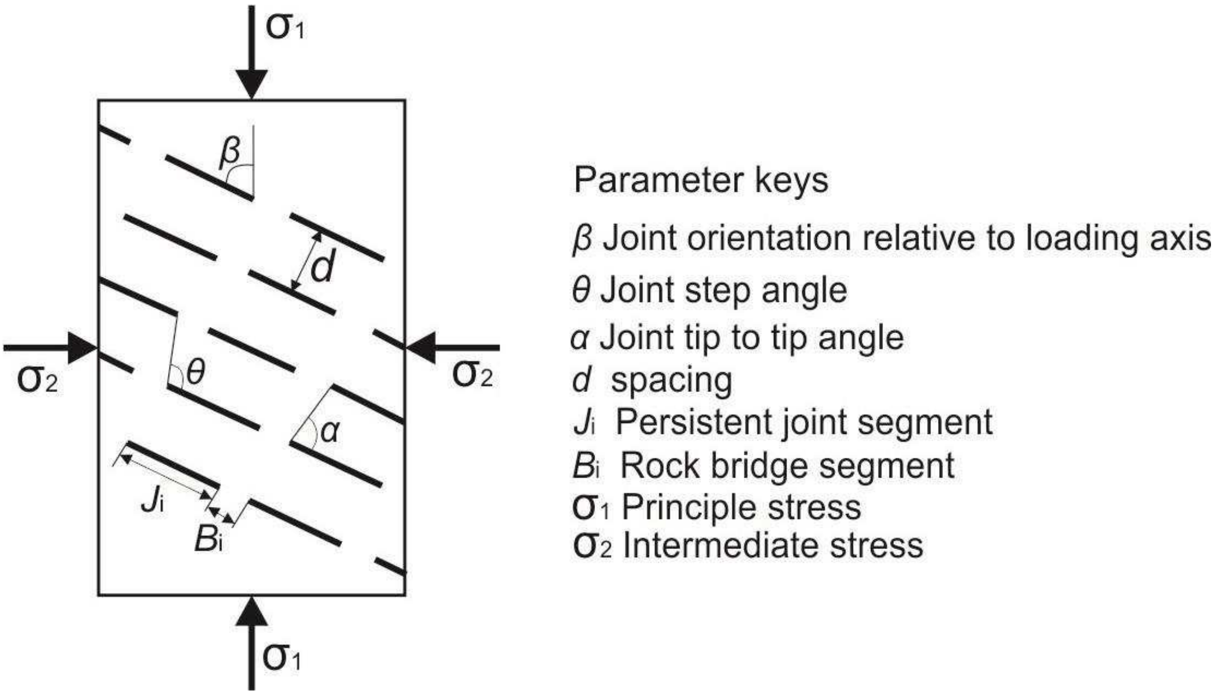
σ1
β
d
θ
α
Ji
Bi
σ2
σ2
σ1
Parameter keys
β Joint orientation relative to loading axis
θ Joint step angle
α Joint tip to tip angle
d spacing
Ji Persistent joint segment
Bi Rock bridge segment
σ1 Principle stress
σ2 Intermediate stress

Fig 11

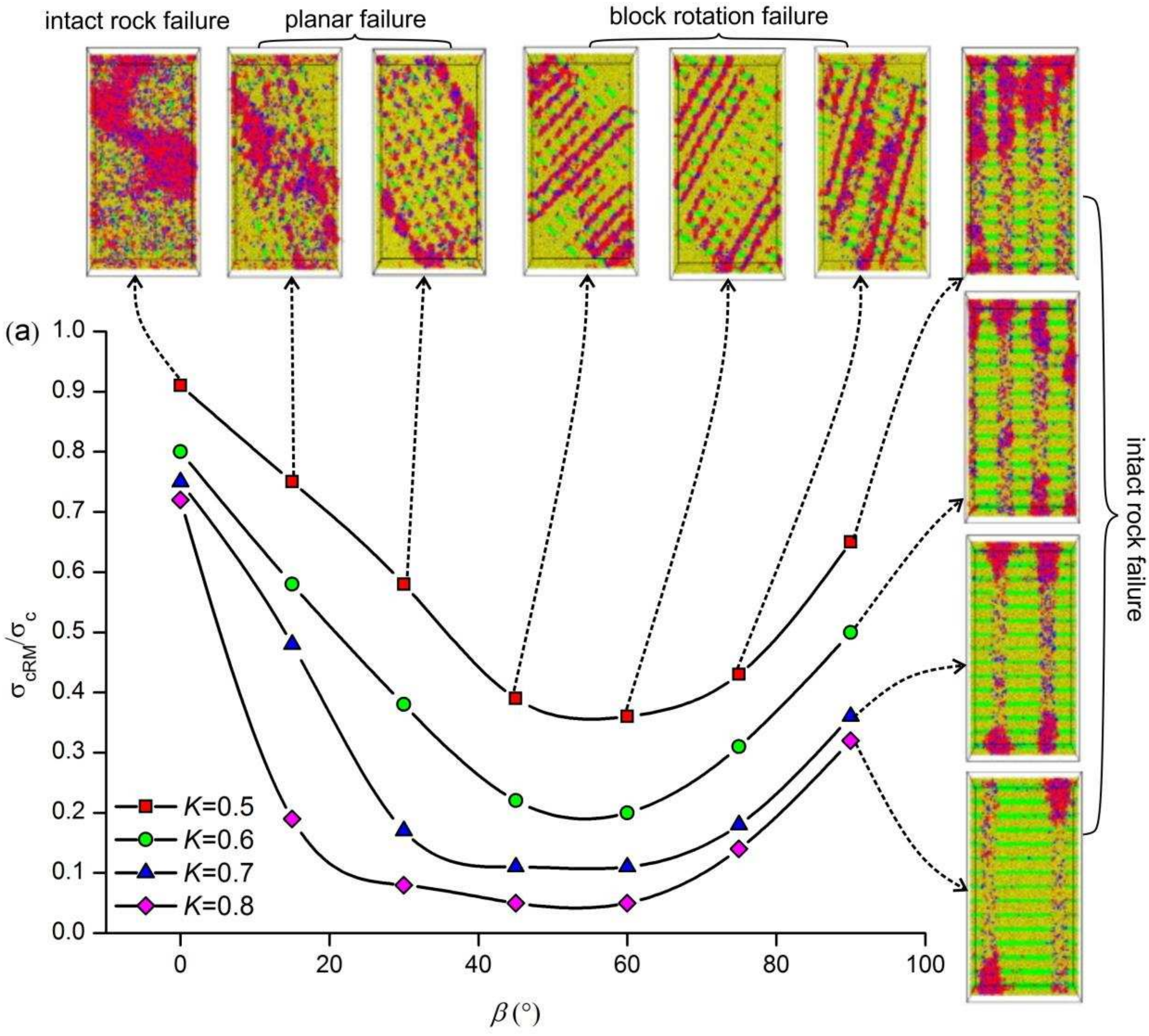

1052

1053 Fig 12a

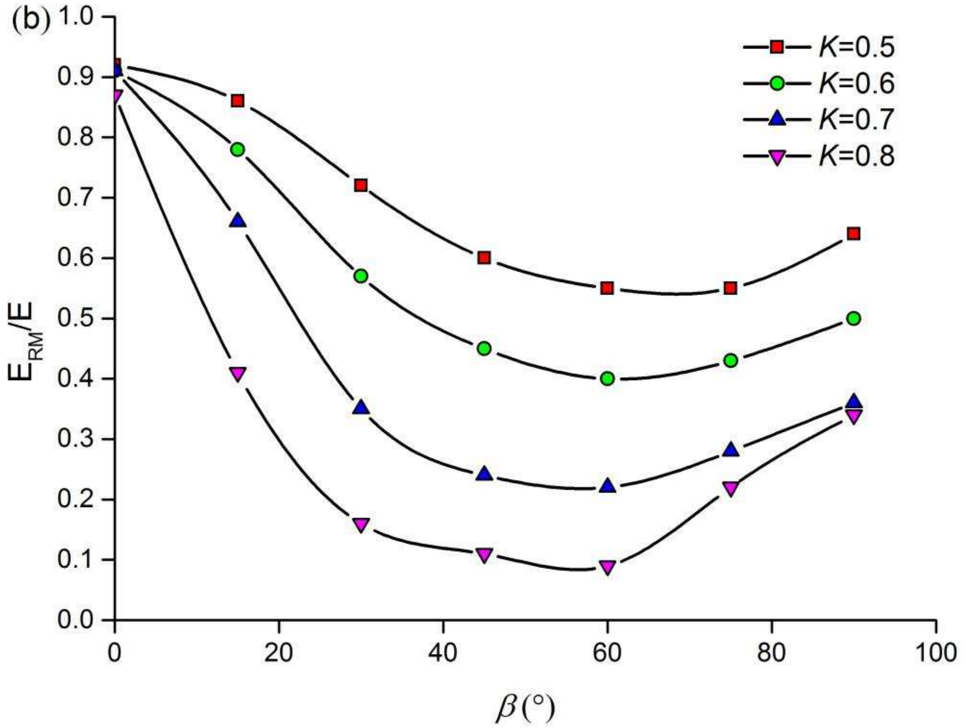
(b)
1.0
0.9
0.8
0.7
0.6
0.5
0.4
0.3
0.2
0.1
0.0
E_{RM}/E
0
20
40
60
80
100
$\beta(°)$
K=0.5
K=0.6
K=0.7
K=0.8

Fig 12b

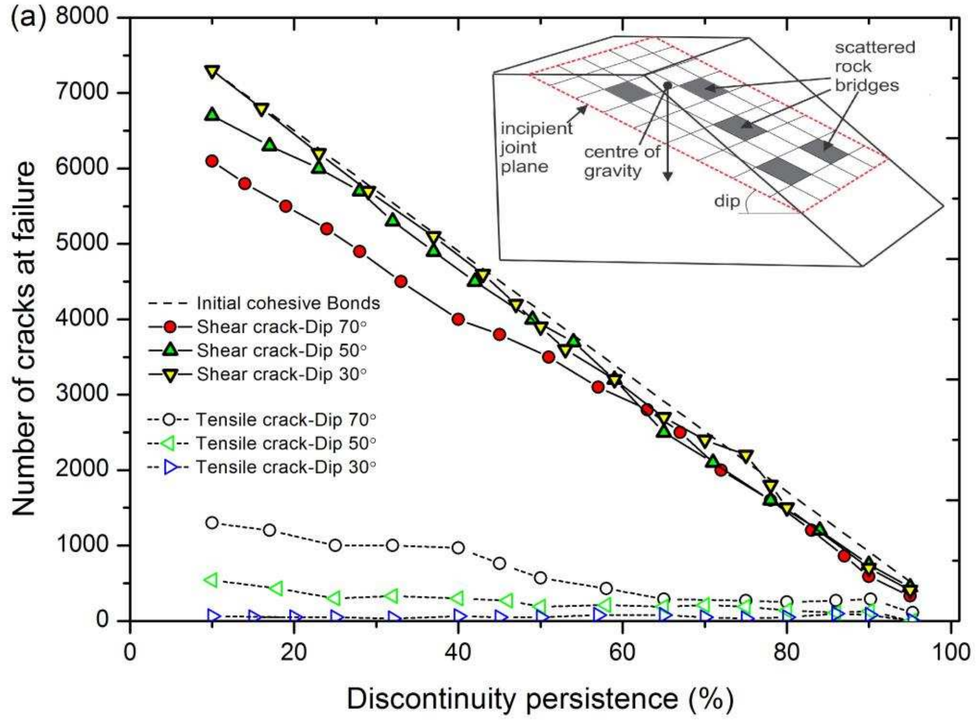
(a)
Number of cracks at failure
Discontinuity persistence (%)
0
1000
2000
3000
4000
5000
6000
7000
8000
0
20
40
60
80
100
scattered
rock
bridges
incipient
joint
plane
centre of
gravity
dip
Initial cohesive Bonds
Shear crack-Dip 70°
Shear crack-Dip 50°
Shear crack-Dip 30°
Tensile crack-Dip 70°
Tensile crack-Dip 50°
Tensile crack-Dip 30°

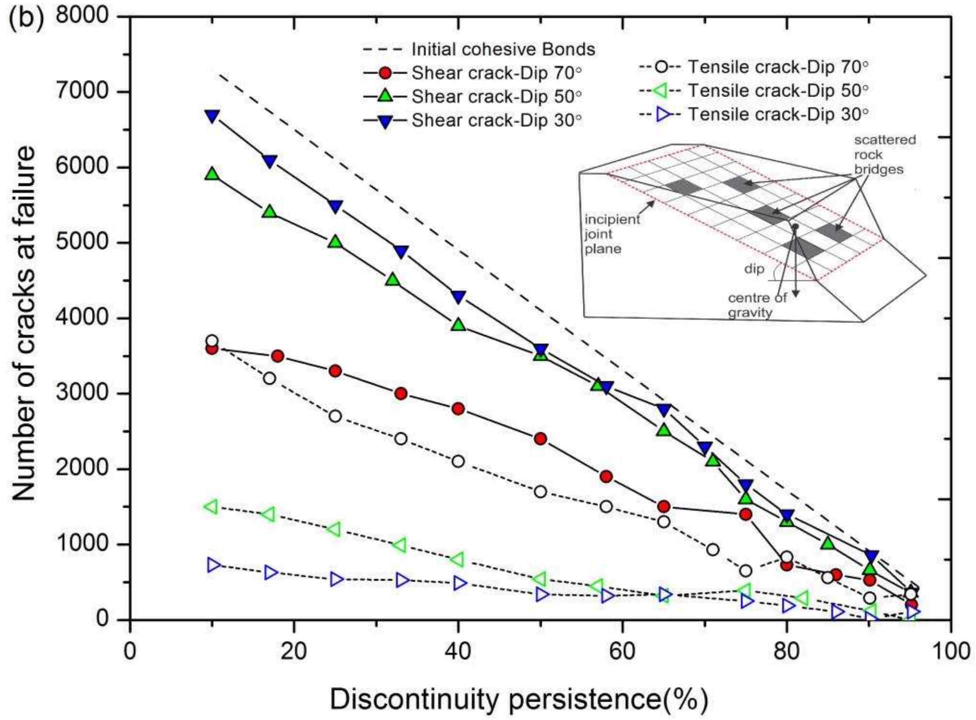
(b)
Initial cohesive Bonds
Shear crack-Dip 70°
Shear crack-Dip 50°
Shear crack-Dip 30°
Tensile crack-Dip 70°
Tensile crack-Dip 50°
Tensile crack-Dip 30°
scattered rock bridges
incipient joint plane
dip
centre of gravity
Number of cracks at failure
Discontinuity persistence(%)

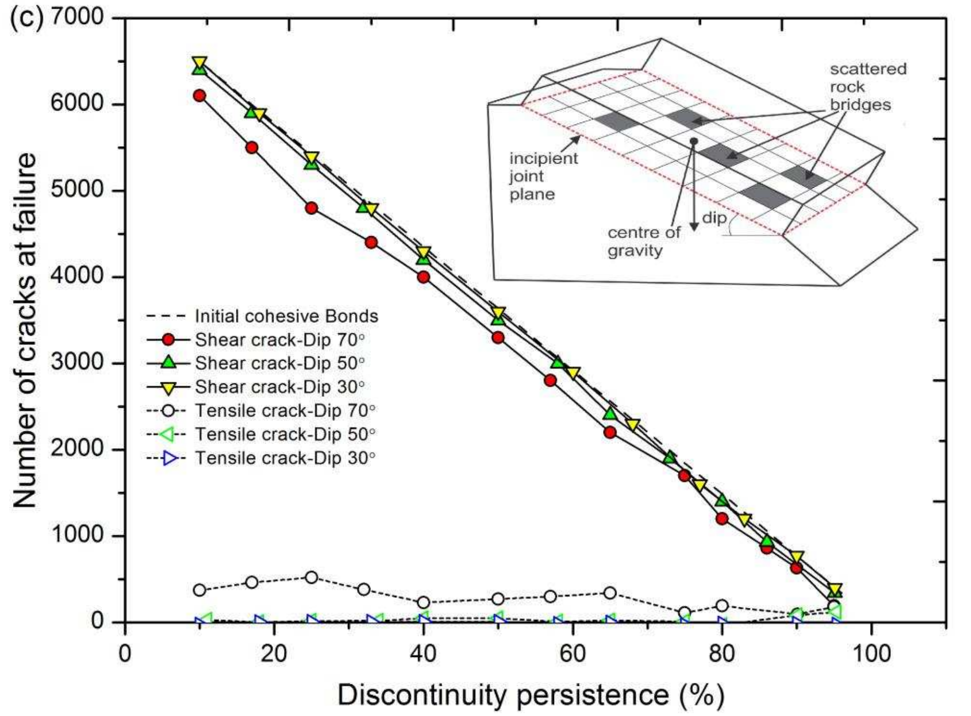
(c)
scattered rock bridges
incipient joint plane
centre of gravity
dip
Initial cohesive Bonds
Shear crack-Dip 70°
Shear crack-Dip 50°
Shear crack-Dip 30°
Tensile crack-Dip 70°
Tensile crack-Dip 50°
Tensile crack-Dip 30°
Number of cracks at failure
Discontinuity persistence (%)

Fig 13

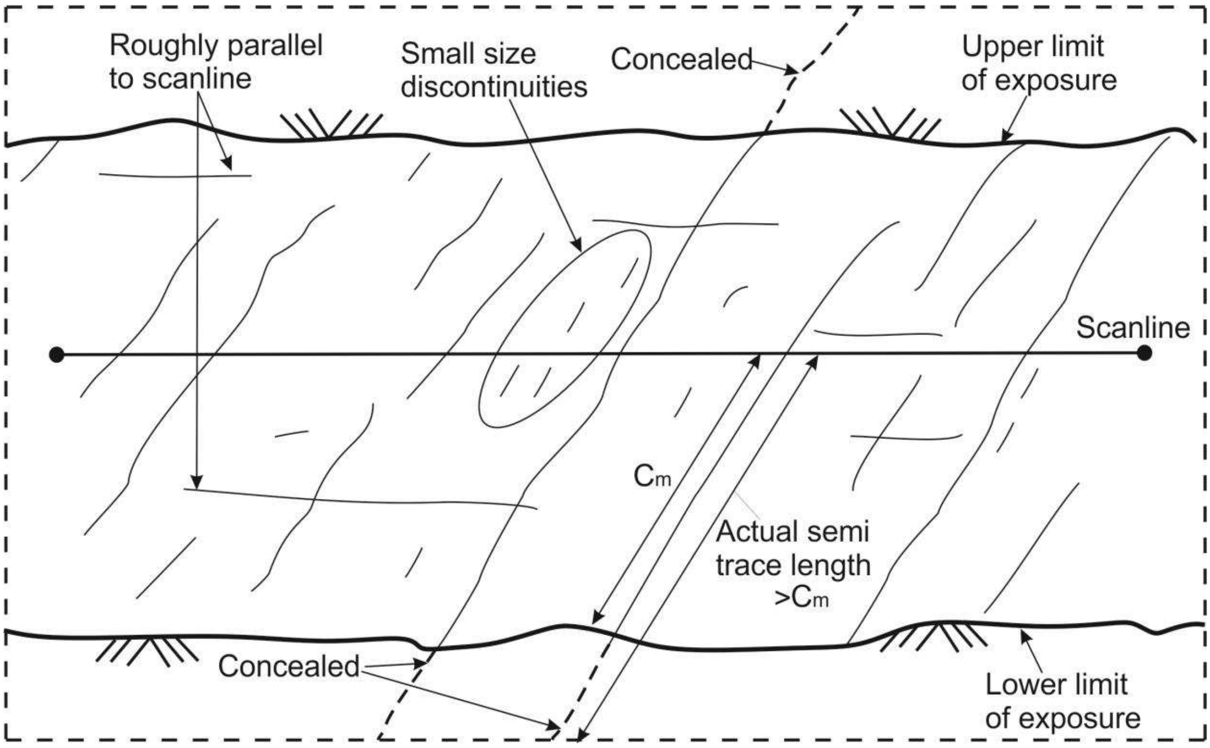
Roughly parallel
to scanline
Small size
discontinuities
Concealed
Upper limit
of exposure
Scanline
Cm
Actual semi
trace length
>Cm
Concealed
Lower limit
of exposure

Fig 14

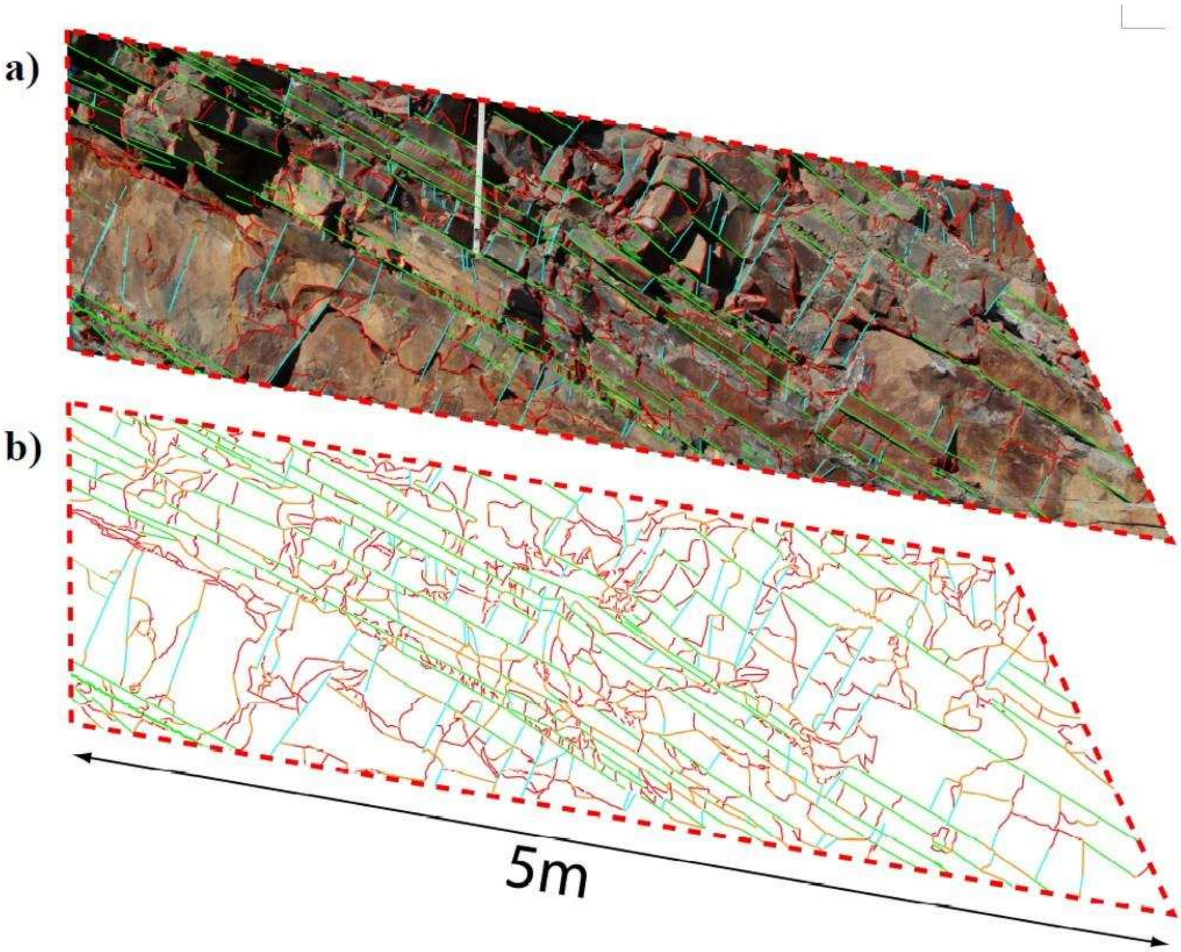

1065

1066 Fig 15

1067

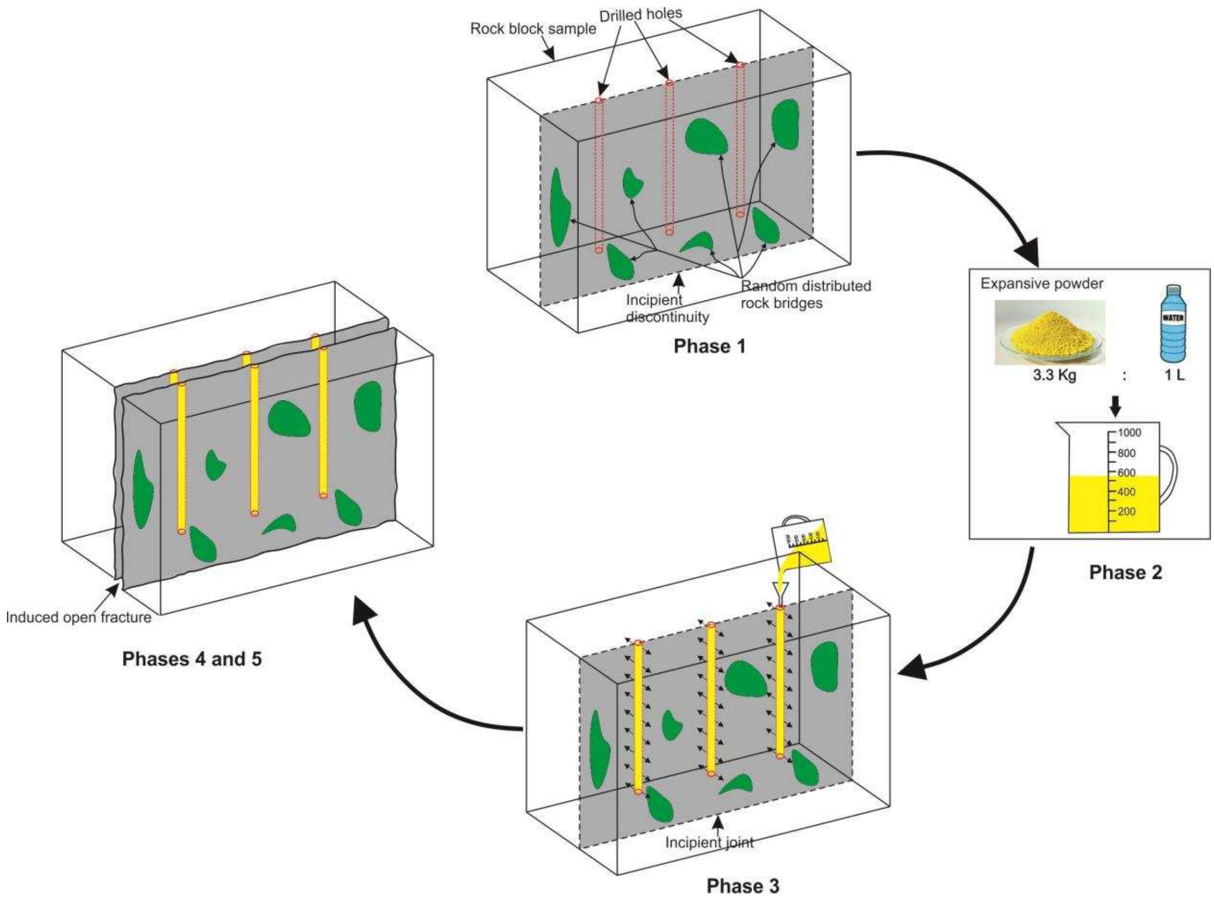

1068

1069 Fig 16

1070

1071

1072

1073

1074

1075

1076

1077

1078

1079

1080

Table 1 Representative contributions to discontinuity size (trace length) estimation from censored measurements.

Methodologies	Major contributions	Remarks	Sampling methods	References
Censored exponential distribution	Field procedure was devised to provide a method for characterizing and estimating trace length. Data requirements dramatically reduced.	The analysis does not consider type of discontinuity termination and tends to overestimate larger trace length.	SS	Cruden 1977
Moment estimate	Moment estimation of unconditional radius distribution of joints was presented.	Reliability of results depends on the probability function assumed.	SS	Baecher and Lanney (1978)
Probability distribution analysis	Four simple probability distributions were used to study bias in scanline sampling. The relations between these distributions provide analytical methods of estimating mean discontinuity trace length.	Reliability of results depends on the probability function assumed.	SS	Priest and Hudson (1981)
Probability distribution function	A technique was proposed for estimating mean trace length on infinite exposures. Does not require lengths and density function of observed traces.	Only applicable to discontinuities whose orientation is described by a probability distribution function.	WS	Kulatilake and Wu (1984)
Distribution-free methods	Simple estimators were developed for the estimation of variably oriented fracture trace length as well as trace density.	Reliability of results depend on the probability function assumed; underlying distribution of trace length is generally unknown.	WS	Mauldon (1998)
Probability analysis, numerical and analytical methods	Joint trace length distribution was estimated for the Poisson disc joint model. Joint diameter distribution was also numerically and analytically investigated	Relies on the assumption that joint lengths are similar in strike and dip directions.	WS	Song and Lee (2001)
Stereological relation analysis	Stereological analysis used to estimate size distributions of elliptical discontinuity from true trace length distribution.	Discontinuity assumed planar and elliptical in shape.	SS and WS	Zhang and Einstein (2002)
Maximum likelihood method	Extends previous methods to include arbitrary joint set and sampling plane orientations.	Derived results only apply for joint traces normal to top and bottom of sampling window.	WS	Lyman (2003)
Statistical graphical approach	A flexible method for inference of trace length using statistical graphical model based on observations at rock outcrops.	--	WS	Jimenez-Rodriguez and Sitar (2006)

Probability weighted moments (PWM) and L-moments	A distribution-free method to estimate fracture trace length distributions in the light of the estimation of PWM and L-moments of true trace length.	--	WS	Li et al. (2014)

SS: Scanline Sampling; WS: Window Sampling